REVIEW

Recent advances in electroless-plated Ni-P and its composites for erosion and corrosion applications: a review

Eman M. Fayyad[1] · Aboubakr M. Abdullah[1] (iD) · Mohammad K. Hassan[1] · Adel M. Mohamed[2] · George Jarjoura[3] · Zoheir Farhat[3]

Abstract

The metallic coating of surfaces plays a vital role in the protection of most industrial applications. Coatings can be carried through various routes (e.g., mechanical and electrochemical plating techniques). Electroless nickel coatings present unparalleled properties and a unique combination of corrosion and wear resistance features. Recently, the use and development of electroless nickel-phosphorus (ENP) coatings has attracted broad attention from many industries (e.g., oil and gas) due to their superior corrosion and wear resistance properties. In the present review article, mechanisms of ENP and preparation methods are briefly outlined. The review sheds light on properties of electroless Ni-P coatings and of their nanocomposites with an emphasis on new products and on their future development.

Keywords Electroless Ni-P · Mechanism · Corrosion · Wear · Composite coatings

1 Introduction

Corrosion is one of the major problems especially in the oil and gas industry. Therefore, pipelines, tanks, and similar equipment require regular maintenance because of corrosion and its associated problems. Consequently, the need for improving the corrosion protection of the metals has motivated the researchers to find superb new coatings or modify the existing ones. Electro, electroless, and mechanical plating in addition to hot dipping are the most frequently used techniques for metallic coatings. However, the unique properties of the electroless-plated coatings and the easiness of the handling process make this type of plating the most marketable method.

Electroless Ni-P (ENP) coatings represent over 95% of industrial electroless coatings. Generally, depending on phosphorus content levels, electroless Ni-P coatings are divided into three categories: low, medium, and high P at 1–7 wt%, 7–10 wt%, and 10–12 wt%, respectively. High phosphorus content Ni-P coating is known for its excellent wear and corrosion resistance. The metallurgical properties of alloys are also dependent on percentages of phosphorus. More studies have been conducted on electroless Ni-P nanocomposites in recent decades. Ni-P-SiC, Ni-P-TiO$_2$, Ni-P-Al$_2$O$_3$, and Ni-P-CNT are successful examples that have attracted attention owing to the improved properties relative to the original Ni-P coatings.

This critical review article will not only help researchers to recognize the recent developments in ENP and metallic composite coating development, but it also recommends the conditions to be considered to enhance the applications of this type of coating in the erosion and corrosion fields. The article includes a comparison between the recent work that took place in the last 5 years, including the used nanoparticles and metals in the ENP composites, the bath conditions, and the used techniques in addition to highlighting the new technologies that are being used.

✉ Eman M. Fayyad
  emfayad@qu.edu.qa

✉ Aboubakr M. Abdullah
  abubakr2@yahoo.com

1   Center for Advanced Materials, Qatar University, P.O. Box 2713, Doha, Qatar

2   Department of Metallurgical and Materials Engineering, Faculty of Petroleum and Mining Engineering, Suez University, Box 43721, Suez, Egypt
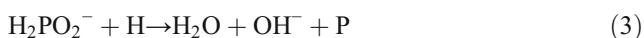
3   Department of Process Engineering and Applied Science, Materials Engineering Program, Dalhousie University, Halifax, Nova Scotia B3J 2X4, Canada

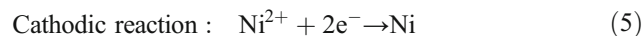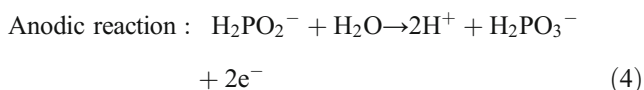## 2 Mechanism of the electroless deposition of Ni-P coatings

Although Wurtz [1, 2] was the first to electrolessly deposit nickel in 1844 through the reduction of Ni^{2+} ions to metallic porous nickel (Ni), his discovery has not attracted considerable attention due to poor and rough coating properties. In 1946, Brenner and Riddel [3, 4] developed formulations and experiments on EN that yielded excellent coatings in terms of shapes and properties. Ever since, electroless deposition of Ni-P (ENP) application has expanded in several industrial areas [5–10].

Gould et al. and others [11–13] explained the kinetics of electroless Ni-P coatings, which are mainly based on the formation and adsorption of atomic hydrogen capacities by a metal surface followed by the reduction of Ni^{2+} and hypophosphite ions and the codeposition of nickel and phosphorus onto a metal surface. Chemical reactions of electroless Ni-P deposition can be described as shown in Eqs. (1–3).

First, hypophosphite ions react with water, Eq. (1), producing atomic hydrogen which is then adsorbed onto the metal surface. The atomic hydrogen produced reduces nickel and hypophosphite ions present in the bath, forming codepositing nickel-phosphorus (Ni-P), Eqs. (2 and 3). Then, the adsorption of atomic hydrogen into the formed Ni-P deposit occurs, followed by the new codeposition of Ni and P. Finally, the H_{ads} produced is consumed, and Ni and P are codeposited.

$$H_2PO_2^- + H_2O \rightarrow H^+ + H_2PO_3^{2-} + 2H \tag{1}$$

$$Ni^{2+} + 2H \rightarrow Ni + 2H^+ \tag{2}$$

$$H_2PO_2^- + H \rightarrow H_2O + OH^- + P \tag{3}$$

The electrochemical mechanism by which Ni-P plating occurs is outlined as follows. It is assumed that hypophosphite ions are catalytically oxidized while nickel and hydrogen ions are reduced along the catalytic surface.

$$\text{Anodic reaction}: \quad H_2PO_2^- + H_2O \rightarrow 2H^+ + H_2PO_3^-$$
$$+ 2e^- \tag{4}$$

$$\text{Cathodic reaction}: \quad Ni^{2+} + 2e^- \rightarrow Ni \tag{5}$$

$$2H^+ + 2e^- \rightarrow H_2 \tag{6}$$

Generally, some reactions of the ENP bath can be unfavorable to deposition. Hypophosphite reactions with water can form molecular hydrogen rather than atomic hydrogen, which minimizes the reducing power and which is deleterious for deposition. In addition is the precipitation of nickel as nickel orthophosphite can reduce concentrations of nickel in the bath. Moreover, orthophosphite can deposit on the coating, creating a rougher coat [14]. These difficulties lead to a reduction in the efficiency of EN coatings. To overcome these issues, a complexing agent must be added to prevent the precipitation of Ni^{2+}. Organic acids such as tartaric, succinic, and maleic acid can be used for this purpose. In addition, adipic and succinic acid can be added to lag the deposition speed of Ni-P and to obviate the formation of a porous coating [13].

3 Electroless Ni-P bath

The main requirements of the electroless deposition of Ni-P are as follows:

1. Source for Ni^{2+} ions: e.g., nickel sulfate or nickel chloride. The nickel ion accepts electrons from the reducing agent, which is the electron donor, and reduces to nickel metal on the surface of the substrate.
2. Reducing agent: an electron source for the reduction of metal ions. Sodium hypophosphite monohydrate is mainly used as a reducing agent to supply catalytic dehydrogenation active hydrogen atoms to reduce nickel ions to metal and to supply the phosphorus portion of the deposited alloy. The sodium hypophosphite bath creates a Ni-P coating with high CR. The hypophosphite ion has a redox potential of − 0.5 V. Therefore, theoretically speaking, it considerably reduces nickel ions (− 0.25 V) under standard conditions [15, 16].
3. Complexing agents are organic acids or their salts (acetic, malic, succinic, or citric) added to control reactions and to prevent solution decomposition, i.e., they prevent the formation of excess free metal ion concentrations. The plating rate is inversely proportional to the complexing ion's stability constant [17]. Complexing agents also act as buffers and retarders for the precipitation of nickel phosphite. The complexing agent used significantly affects the quality of the deposits and internal stress and porosity levels.
4. Stabilizers or accelerators are added in small amounts (ppm) to increase the deposition rate and to weaken the bond between hydrogen and phosphorus atoms in hypophosphite molecules to facilitate the adsorption of phosphorus onto the catalytic surface. Pb, Sn, As, Mo, Cd, and Th ions, malic, and thioureas are examples of popular stabilizers. Succinic acid is the chemical most frequently used as an accelerator.
5. Temperature is energy for deposition and is considered to be an important variable of an electroless bath. As it affects kinetics and rates of deposition, it must be controlled for high quality coating. The deposition of electroless Ni-P coatings occurs at temperatures of 60 °C and above. As the temperature increases, the plating rate increases exponentially [18]. A low temperature results in a reduction of energy, causing the deposition rate to decrease as well. On the other hand, a very high temperature renders the bath

extremely active, leading to bath instability. The optimum operating temperature of an acid hypophosphite plating solution ranges from 85 to 90 °C. When temperatures increase beyond 90 °C, the phosphorus content of the deposit decreases and the potential for solution decomposition will increase [19].

6. pH regulator is used to adjust pH with deposition time as sodium hydroxide or sulfuric acid. pH control is an important parameter, as it affects phosphorus content in the deposit, i.e., a higher pH value lessens in the phosphorus content in the deposit and vice versa. Chen et al. concluded that phosphorus content levels increase to 25% at pH 4, while the percentage of phosphorus content decreases to 1% in an alkaline range [20].

   3.A. Electroless nickel-phosphorus acidic bath

According to Brenner and Riddell [3], acid electroless nickel-phosphorus baths present advantages over alkaline baths, exhibiting high levels of composition stability as there is no loss of complexant by evaporation, high levels of deposition and thickness, and high quality coatings. When using an acid electroless nickel bath, it is easy to control the percentage of phosphorus content in the deposit, which is the main factor that controls a deposit's properties. Upon being heated, the bath does not decompose, i.e., it is thermally stable [21]. Therefore, acid solutions are prioritized in several industries, and especially in corrosion applications.

   3.B. Electroless nickel-phosphorus alkaline bath

In contrast to an acid bath, an alkaline bath is unstable at higher temperatures. A sudden decrease in bath pH occurs due to a loss of ammonia, which is added to raise the pH of the bath at a high temperature. Hence, bath pH is very difficult to control at temperatures above 90 °C. Furthermore, the rate of nickel deposition is directly proportional to the hypophosphite concentration. As an increase in hypophosphite levels leads to bath instability due to homogeneous deposition in the bulk, alkaline bath deposits ensure lower levels of corrosion

resistance and adhesion. They thus cannot yield a thick coating or plate steel or other metals [21].

4 Heat treatment effects

The heat treatment is a vital factor that clearly affects the most properties of ENP coatings and structures. An as-deposited film of ENP undergoes structural changes when it is heat treated at different temperatures [22]. EN-P crystallization behaviors can be divided into (i) an alloy that contains microcrystalline nickel as a prime constituent in the deposited state and (ii) an alloy that only accommodates the amorphous phase and that does not contain microcrystalline nickel as a prime constituent. It is reported to invariably decrease the corrosion resistance of electroless coatings. When an ENP is composed of 10.8% P and has a microcrystalline structure as a major constituent, it is annealed at a temperature of 200 to 300 °C for 4 h. This results in the formation of $Ni_{12}P_5$ microcrystalline nickel and in Ni_3P phases at all temperatures. Crystalline nickel and Ni_3P phases are observed under annealing at higher temperatures (400–600 °C) [23].

Heating a Ni-P coating at temperatures of between 300 and 400 °C for 1 h increases hardness levels due to the formation of nickel phosphide (Ni_3P) as is shown in Fig. 1 [24]. The hardness is reduced beyond 400 °C due to the formation of lattice defects and with the coarsening of Ni_3P particles [25]. Zhao et al. investigated the effects of low temperature annealing on the properties of amorphous Ni-P alloys over different periods [26]. It was found that levels of microhardness initially decreased and then increased with annealing time. In addition, heat treatment has obvious effects on wear resistance [27], conductivity, and resistivity levels [28] and on frictional properties [29]. Nava et al. investigated the effects of heat treatment at higher temperatures (500–600) on the corrosion resistance of Ni-P coatings (10.6% P). It was found that the

Fig. 1 Effects of heat treatment temperature on the hardness of nickel-phosphorus coatings [24]
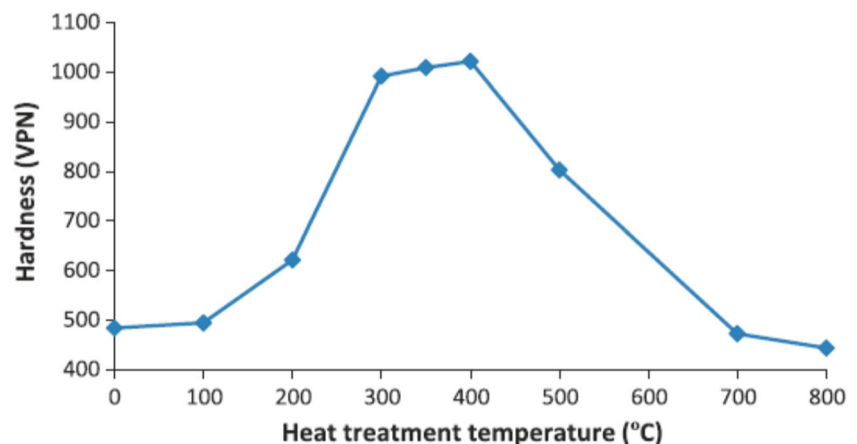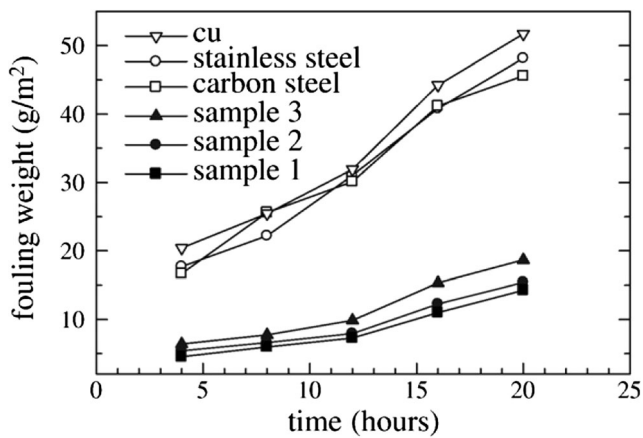
Fig. 2 Fouling adhering weight versus time of immersion in boiling water for different surfaces. Samples 1 (amorphous), 2, and 3 (nanocrystalline with different percentages) [51]

corrosion resistance decreased as the annealing temperature increased [30].

4.1 Electroless Ni-P composite coatings

Electroless nickel composite coatings are products of codepositing particulate substances found in an electroless Ni-P bath. These substances are found in powdered form and are either hard or dry lubricants. Silicon carbides, diamonds, aluminum oxides, and tungsten are examples for hard materials [31, 32]. Lubricant materials are similar to fluoropolymers, molybdenum disulfide, and graphite [33]. Such materials are added to enhance the quality of electroless Ni-P coatings by improving their wear resistance by reducing their friction coefficient. At first, electroless Ni-P composite coatings were not successfully prepared, as the presence of fine particles increases the surface area of a bath, resulting in instability. Later, suitable stabilizer was added to address this challenge and electroless Ni-P
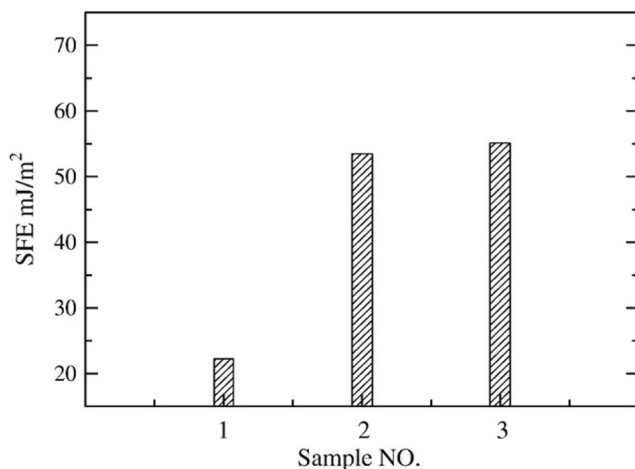

Fig. 3 Surface free energy of samples 1 (amorphous), 2, and 3 (nanocrystalline with different percentages) [51]

composite coatings have been prepared easily. Durable composite coatings necessitate high integrity between particles and an electroless Ni-P bath matrix.

Some key conditions are required to increase the quality of electroless Ni-P composite coatings (e.g., bath stability, agitation, particle size, concentration, and types of surfactant used). Thiourea and maleic acid improve the stability of a bath and extend its life. Agitation plays an essential role in preventing the rotation of hard particles such as diamonds and silicon carbide in a suspension and it is recommended that their surfaces be oriented upward to be easily occluded in the deposit [34].

The size and concentration of particles are pivotal elements shaping the distribution of particles in a deposit. These particles must be of a suitable shape and size, must be insoluble in a given solution, must be free of contaminants, and must be suspended in the bath [15]. Suitable particle concentrations should be used to prevent their agglomeration [35, 36]. Each composite has different properties that are dependent on many factors. For example, the addition of 20–25 vol% SiC to an ENP bath increases the hardness of electroless composites, whereas the addition of the same percentage of polytetrafluoroethylene (PTFE) reduces hardness levels. The selection of a suitable surfactant plays a major role in the incorporation of soft particles such as PTFE [37, 38]. Mafi et al. found that acetyl trimethyl ammonium bromide (AcTAB) and polyvinylpyrrolidone (PVP) as surfactants yield a uniform distribution of PTFE particles in ENP coatings, whereas sodium dodecyl sulfate (SDS) does not [39].

Many key studies have been conducted the synthesis of nanocomposite coatings such as SiC [40], TiO_2 [41], CeO_2, [42], Al_2O_3, $ZnSnO_3$, $ZnSiO_3$ [43], and nanometer diamonds (NDs) [44]. Recently, a new means of generating nanocomposite coatings such as SiO_2, CNT, ZrO_2–Al_2O_3–Al_3Zr, hexaferrites, ferrites, ZnO, and Al_2O_3–TiO_2 has attracted considerable attention. Furthermore, shape memory alloys such as TiNi and novel nanoparticles exhibit a combination of novel properties such as shape memory effects, super-elasticity, biocompatibility, and high damping capacity levels [45–47]. In the following section, properties and recent developments related to ENP and its composites are presented.

5 Properties of ENP and composite coatings

5.1 Microstructure

The properties of ENP coatings are mainly dependent on the content of phosphorus that controls their microstructures. The microstructure of ENP coatings has been reported to be either amorphous or crystalline or both depending on the phosphorus content involved. Crystalline (β), mixed amorphous crystalline (β and γ coexist) and amorphous (γ) structures have

Fig. 4 SEM micrographs of the samples: **a** 3003 bare substrate, **b** electroless nickel plated on 3003 substrate for 90 min, **c** sprayed Al–Ce coating, and **d** electroless nickel plated on the sprayed Al–Ce coating for 90 min [52]
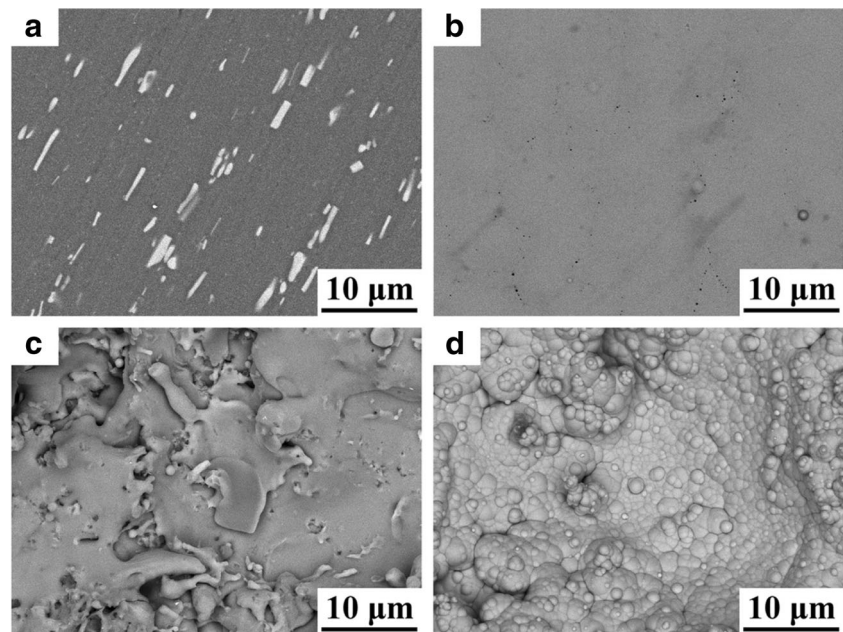
been reported for low (1–5 wt%), medium (6–9 wt%), and high (10–13 wt%) P ENP coatings, respectively. Amorphous structures (γ) can be crystallized through heat treatment. The more the P content in the ENP coating, the higher the corrosion resistance will be.

Many factors affect degrees of crystallinity besides phosphorus content levels, e.g., heating rates, heat treatment temperatures, and the timing of heat treatment. Zhang and Yao intensively studied effects of heat treatment on the transformation of ENP coating microstructures from amorphous to crystalline [48]. Incorporated particles such as CeO_2 and TiO_2 did not have any effect on

the structure of the ENP matrix [49]. Others such as SiC and B_4C have been found to change the orientation of nickel crystallite [50].

One study [51] showed that the γ phase of the ENP deposit exhibits the best anti-fouling properties relative to nanocrystalline phases, uncoated Cu, stainless steel, and carbon steel substrates, Fig. 2. Furthermore, it was found that the amount of nanocrystalline phase in the ENP deposit affects the surface free energy level, Fig. 3, in addition to changing the anti-fouling and corrosion resistance of the deposit. The nanocrystalline phase in the Ni-P coating deteriorates the corrosion resistance of the deposit while the amorphous Ni-P coating

Fig. 5 SEM micrographs of the samples after immersion corrosion for 24 h: **a** 3003 bare substrate, **b** electroless nickel plated on 3003 substrate for 90 min, and **c** electroless nickel plated on the sprayed Al–Ce coating for 90 min [52]
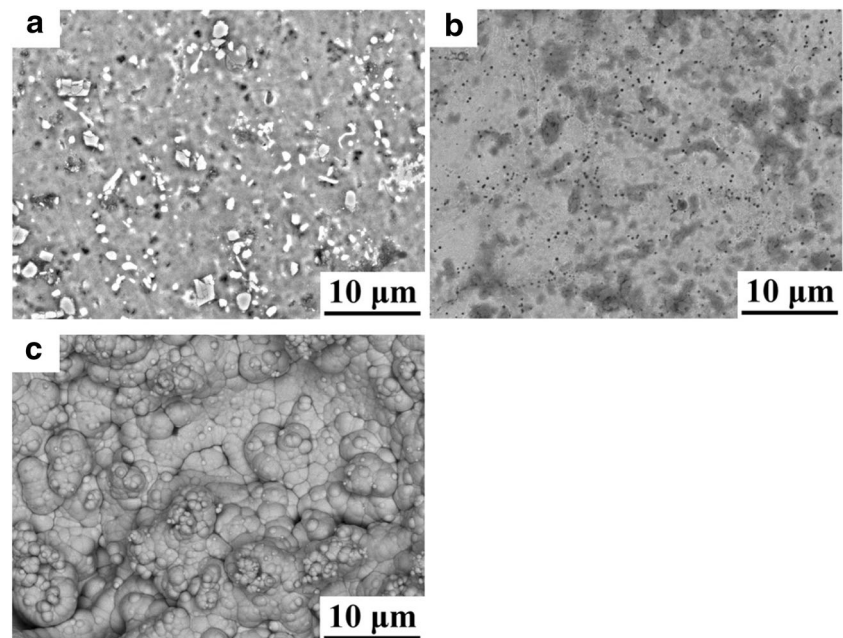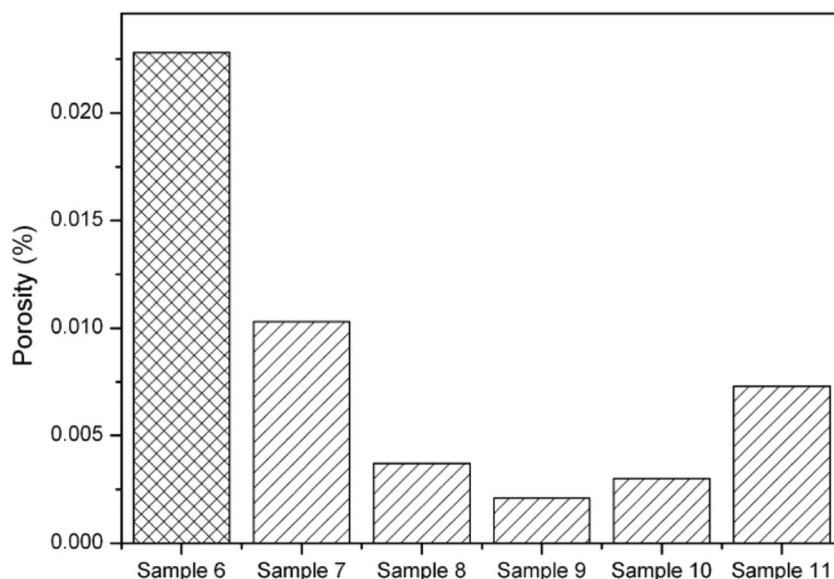
Fig. 6 Porosities of the single-(sample 6) and three-layer coatings (Ni-P/Cu/Ni-P), samples 7–11, for different deposition times [56]

increases corrosion resistance and anti-fouling properties. This is attributed to the homogeneity of its structure, which does not contain any structural defects or grain boundaries.

In 2015, Hejie Yang [52] illustrated differences in surface morphologies, microstructures, and chemical composition distributions between the amorphous ENP layer deposited directly onto an Al 3003 alloy and that deposited onto an interlayer of sprayed Al-Ce coating. Their results show that this type of ENP coating has a circinate structure with cauliflower-like nodules and includes almost no micro-pores on its surface, thus supporting a higher degree of corrosion resistance that is superior to that of conventional electroless ENP coatings as is shown in Figs. 4 and 5.

Several studies on different effects of the microstructure of ENP and of its composite coating include [53–55].

5.2 Porosity

The porosity of ENP coatings is an indicator of coating quality. Adhesion and corrosion resistance levels are dependent on porosity levels. The presence of open pores in a coating results in severe levels of galvanic corrosion, as the pores act as a anode while the coating surface acts as a cathode. The porosity of EN coatings is linked to many parameters such as

roughness/morphology, coating thickness, substrate pretreatment, filtration, and agitation. Under the same surface treatment and thickness conditions, it was found that the porosity of ENP deposits is lower than that of electrodeposited nickel-phosphorus. Moreover, heat treatment and multilayer ENP deposition significantly reduce porosity levels. Thus, ENP deposits are more corrosion resistant than electrodeposited ones.

Multilayers of electroless ENP coatings were prepared by Zhao et al. [56] and were arranged in the following configuration: Ni-P/Cu/Ni-P. The presence of crystalline Cu deposits blocks pores of the three-layer coatings, leading to a decrease in coating porosity and to an increase in corrosion resistance. The highest levels of porosity and corrosion resistance are obtained when the plating time of the Ni-P inner layer is set to 20 min to 40 min. Figure 6 illustrates the porosity of the single layer (sample 6) relative to the porosity of the three layers (samples 7–11). The coated samples and their times of deposition are described as the follows: sample 6 (Ni-P single layer, 60 min), sample 7 (Ni-P inner layer, 10 min/Cu interlayer, 10 min/Ni-P outer layer, 50 min), sample 8 (Ni-P inner layer, 20 min/Cu interlayer, 10 min/Ni-P outer layer, 40 min), sample 9 (Ni-P inner layer,

Table 1 Surface roughness Ra (μm), friction coefficient, and adhesion strength of ENP coatings on Mg, AZ31, and AZ91 substrates [58]

Sample	Ra (μm) Before plating	Ra (μm) After plating (120 min)	Friction coefficient of EN coating	Adhesion strength of EN coating (Lc, N)
Mg	0.20 ± 0.03	0.89 ± 0.06	0.30	8.7
AZ31	0.90 ± 0.06	0.62 ± 0.04	0.20	13.1
AZ91	2.8 ± 0.2	1.85 ± 0.08	0.18	10.1

Fig. 7 Surface morphologies of electroless Ni-P coatings: **a**, **b** without magnetic attrition and **c**, **d** with magnetic attrition [59]
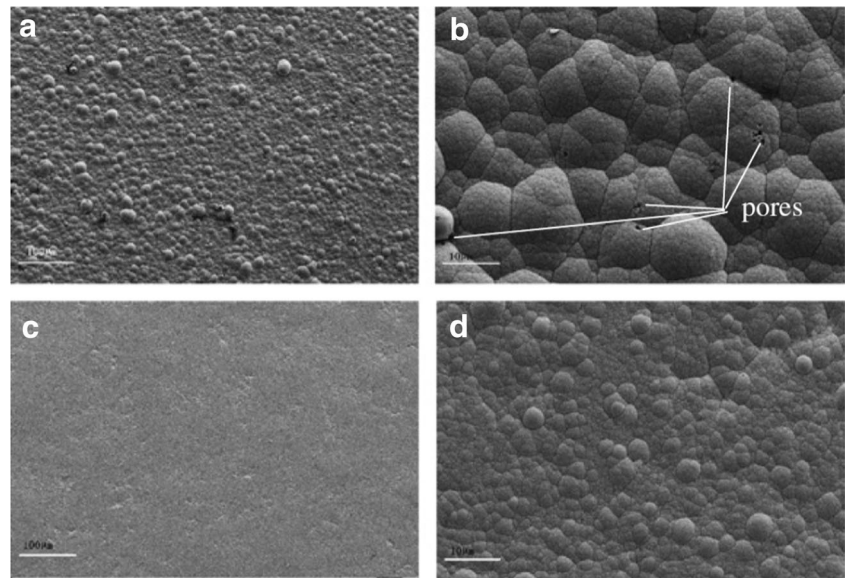
30 min/Cu interlayer, 10 min/Ni-P outer layer, 30 min), sample 10 (Ni-P inner layer, 40 min/Cu interlayer, 10 min/Ni-P outer layer, 20 min), and sample 11 (Ni-P inner layer, 50 min/Cu interlayer, 10 min/Ni-P outer layer, 10 min).

Sadreddini et al. used SiO_2 nanoparticles to form electroless Ni-P-SiO_2 nanocomposite coatings on Mg substrate that enhanced the porosity of the ENP coatings [57]. Different concentrations of SiO_2 were added and examined. It was found that as the concentration of SiO_2 nanoparticles increases, the porosity of the coating decreases. Accordingly, corrosion resistance levels increase to a defined concentration of SiO_2 of 12.5 g L^{-1}. Then, the corrosion resistance starts to decrease with increasing concentrations of SiO_2 nanoparticles to above 12.5 g L^{-1} due to the agglomeration of nanoparticles, which increases the solution viscosity and decreases the deposition rate.

5.3 Adhesion

The stronger a coating's level of adhesion becomes, the more corrosion protection it will ensure. ENP deposits adhere due to the formation of strong metal-to-metal bonds during ENP deposition. ENP coatings have been prepared on Mg metal and on two types of alloys, AZ31 and AZ91, to investigate their friction and adhesion properties [58]. Findings show that the adhesion of these coatings to Mg alloys is greater than that to pure Mg as is shown in Table 1.

Gao et al. [59] illustrated the application of the mechanical attrition technique to a Mg alloy to improve the adhesion, hardness, and corrosion resistance of ENP deposits. Throughout the electroless plating process, coatings were deposited atom by atom, in turn modifying the microstructure of the coatings by moving
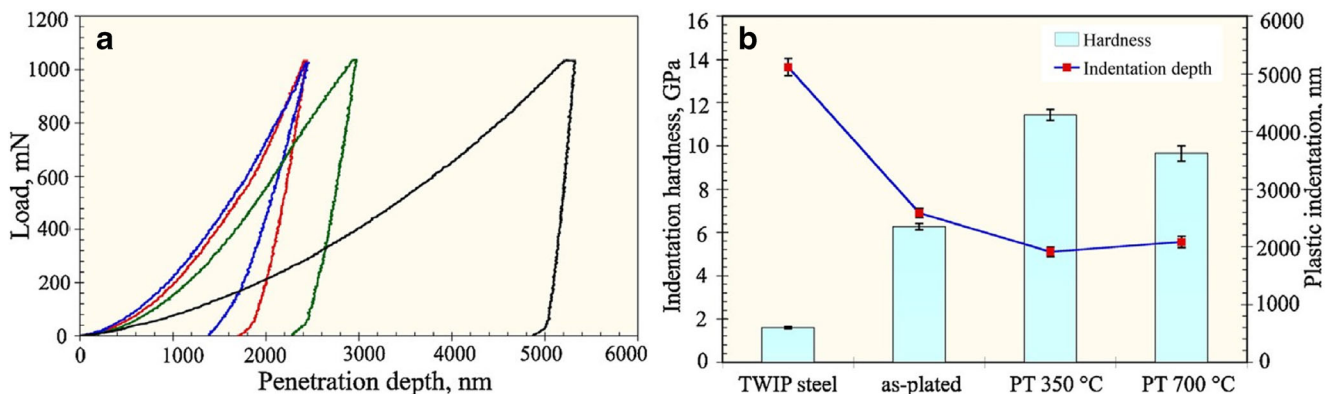

Fig. 8 The results of micro indentation tests conducted on raw TWIP steel substrate (black curve) amorphous/as-plated (green curve) and annealed at 350 °C (blue curve) or at 700 °C (red curve) microstructures at room temperature: **a** load–penetration depth (P–h) curves and **b** indentation hardness and plastic indentation derived from (**a**) [63]
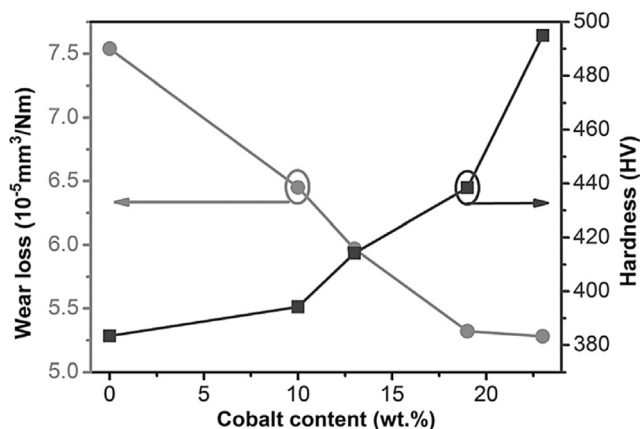
Fig. 9 Hardness and volume loss of five Ni-Co-P/TiN composite coatings with various Co content levels [TiN-free Ni-Co-P, TiN-Ni-Co10-P, TiN-Ni-Co13-P, TiN-Ni-Co19-P, and TiN-Ni-Co23-P] [70]

atoms through low-energy mechanical attrition. An alloy layer at the interface between ENP coatings and Mg alloys formed, leading to the formation of ENP coatings with a smooth, compact, and fine-grained structure free of pores and cracks as is shown in Fig. 7.

5.4 Hardness

The hardness of ENP coatings is mainly dependent on three parameters: phosphorus content, the timing, and temperature of the heat treatment process applied.

Regarding phosphorus content levels, as it increases, the hardness of the ENP coating decreases due to the presence of a large number of soft γ phase microstructures in the high phosphorus coating. Conversely, in low phosphorus coatings, β phase, which is harder than γ phase, is prominent and spurs an increase in hardness levels. Maximum and minimum ENP coating hardness can be achieved when the microstructure includes either β or γ phase only, respectively.

Regarding the temperature and timing of heat treatment, it has been reported that these factors are also affected by phosphorus content levels. When the microstructure of the ENP coating consists of one phase only (phosphorus content levels of below 4.5 or above 11), the optimum heat treatment temperature required to obtain maximum hardness levels is 400 °C for low phosphorus content levels and 330 °C for high phosphorus content levels [60]. Moreover, many sources

report that maximum hardness can be achieved through 1 h of heat treatment at 400 °C [61, 62]. The challenge is to acquire an ENP coating with a high degree of hardness that provides good wear and erosion resistance.

A multilayer of ENP coating was produced on twinning-induced plasticity (TWIP) steel by Hamada et al. [63]. The hardness of the coating was studied under two conditions: as-plated and post-treated (PT) at 350 °C and 700 °C for 1 h, respectively. From Fig. 8, the highest hardness value was found for the PT coating at 350 °C.

Generally, the hardness of ENP composite coatings is higher than that of ENP coatings. The hardness of ENP composite coatings is dependent on the types of particles used (specifically whether they are hard or soft). As the concentration of hard particles such as SiC and Si_3N_4 increases, the coating hardness increases [64]. Increasing the number of soft particles such as PTFE [65] in the composite results in a decrease in coating hardness.

In 2009, Dong et al. studied the hardness, wear resistance, and mechanical properties of $Ni-P-SiO_2$ nanocomposite coatings before and after heat treatment. They found that after heat treatment at 400 °C, the hardness, and resistance of the ENP composite were greatly increased relative to those of the ENP coating [66]. The addition of a small amount of SiC to an electroless Ni-P bath to form Ni-P-SiC composites increased the hardness of the conventional Ni-P coating two-fold (from 4.5 for pure Ni-P to 8.5 GPa for Ni-P/SiC composite coating). In addition, the presence of SiC nanoparticles in the Ni-P matrix acted as a barrier to the corrosive solution and increased the corrosion resistance of the composite [67]. Chen et al. added a transparent layer of TiO_2 to conventional ENP to improve its hardness. The hardness was in turn increased from 710 to 1025 $HV_{0.2}$ and the wear resistance level was improved [68]. Liuhui et al. reported that TiN nanoparticles can considerably improve the hardness of a Ni-P-TiN nanocomposite coating due to its uniform distribution in the Ni-P matrix [69]. TiN nanoparticles are successfully incorporated into the electroless Ni-Co-P coating matrix to form a Ni-Co-P/TiN nanocomposite on the Al substrate. Different weight percentages of cobalt were added to the aforementioned nanocomposite coating [70]. Microhardness levels were in turn enhanced as cobalt content levels in the nanocomposite increased, Fig. 9. Moreover, as is shown in Table 2, adhesion,

Table 2 Comparison of the performance of TiN-free Ni-Co-P and TiN-Ni-Co13-P composite coatings prepared in a solution with $CoSO_4.7H_2O$, 12 $g.L^{-1}$ [70]

Sample	Adhesionforce (N)	Friction coefficient	Hardness ($HV_{0.2}$)	Wear rate (mm^3 Nm^{-1})	E_{corr} (V)	I_{corr} (mA cm^{-2})
TiN-free Ni-Co-P	10	0.392	391	0.019	− 0.69	5.01
TiN-Ni-Co13-P	12	0.414	414	0.022	−0.58	2.88

Fig. 10 Photomacrographs of ENP-coated samples after tensile testing, illustrating extensive fractures in ENP plating: crack rings were observed to be normal to the tensile axis and delamination was found to be quite limited [79]
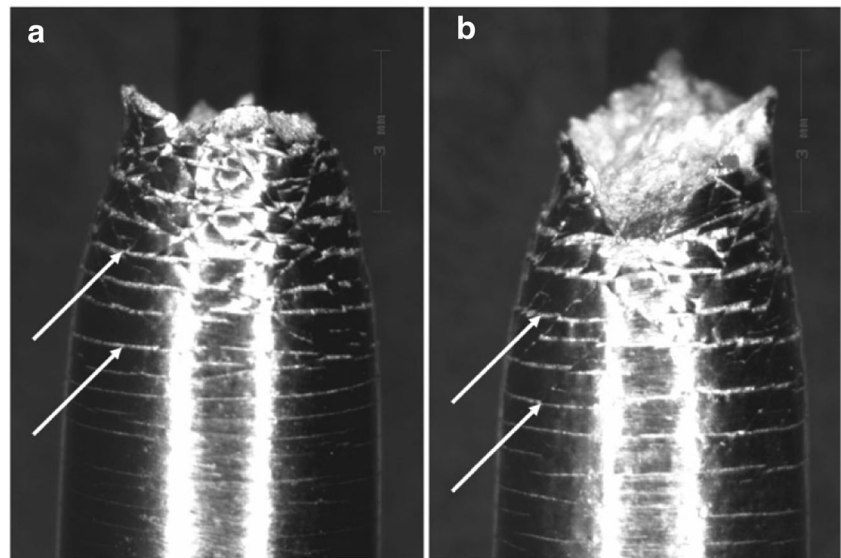
friction coefficient, hardness, wear rates, and corrosion resistance levels were significantly improved when TiN was included in the coating.

Many studies on different composites have achieved improvements in ENP and ENPC coating hardness (for details, see [71–78]).

5.5 Tensile strength

The tensile strength of an ENP deposit is directly related to the phosphorus content and microstructure involved. Increasing phosphorus content levels leads to a high tensile strength. Therefore, an amorphous microstructure has a high tensile strength due to an absence of defects and high stress areas. When a microstructure consists of both β and γ phases, ductility levels are at their lowest values. Lowering phosphorus content levels to less than 4 wt% or increasing them to above 11 wt% increases the ductility of ENP deposits. The high tensile strength of the coating decreases is ductility.

Pineiro et al. [79] examined the tensile strength and fatigue properties of an Al alloy coated with ENP in air and in 3 wt% NaCl solution. The as-deposited coating included 9.5 wt% of P. The coating was found to exhibit strong adherence to a substrate even when it was subjected to tensile stress levels exceeding the yield strength. The ENP coating gave rise to a decrease in the number of cycles to failure (N_f) when it was tested in air and in 3 wt% NaCl solution. The decrease in N_f variation was roughly 56–45% when the coating was tested in air, whereas during testing with the NaCl solution, levels of decline ranged from roughly 65–44%, Figs. 10 and 11.
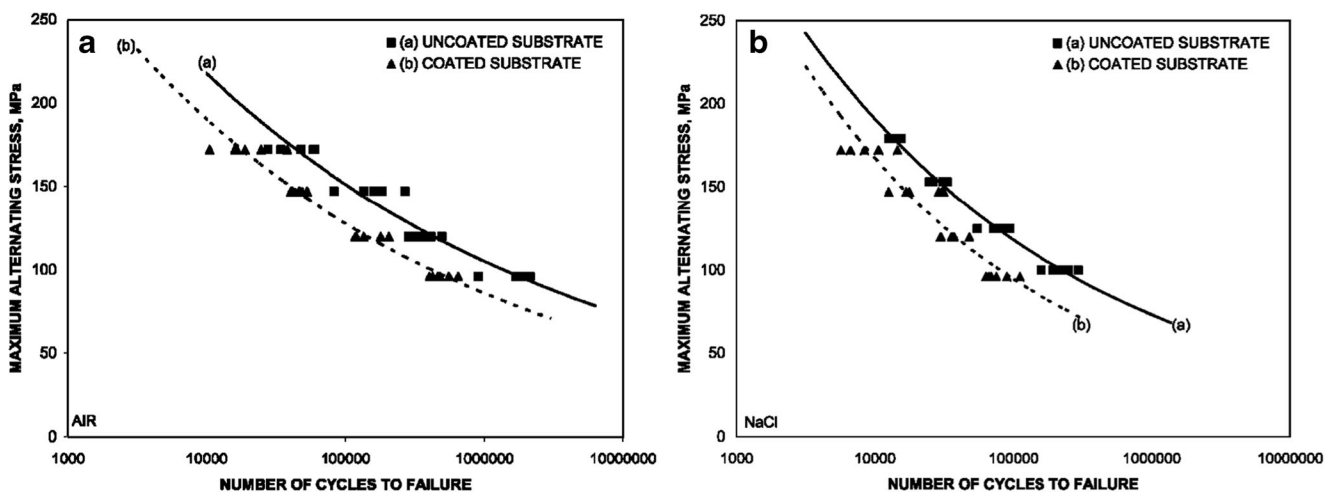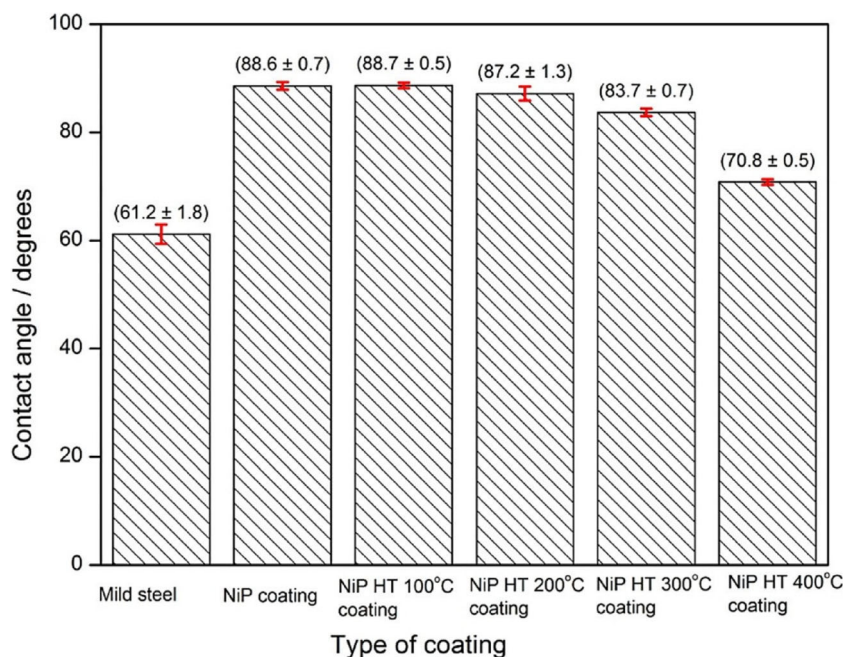

Fig. 11 Mean number of cycles prior to fracturing N_f as a function of alternating stress applied to material S for uncoated and coated specimens tested in **a** air and **b** 3 wt% NaCl solution [79]

Fig. 12 Contact angle measurements of substrate and Ni-P coatings for different heat-treated conditions [87]


5.6 Fatigue properties

The fatigue strength of ENP coatings is a contentious topic among researchers. Generally, ENP deposits reduce the fatigue strength of a substrate under as-deposited conditions and it is decreased even further following heat treatment. Reductions in fatigue strength are mainly based on the composition, heat treatment, and thickness of the coating and on the original fatigue strength of the substrate. Several investigations [80] have shown that ENP coatings weaken substrates. However, others studies have shown an increase in substrate fatigue strength, e.g., Puchi et al. studied the effects of ENP coatings on fatigue properties of AISI 1010 and 1045 substrates. Their results show that ENP coatings, 10 wt% P, improve the fatigue properties of the aforementioned alloy [81]. Puchi et al. also investigated the fatigue and corrosion-fatigue behaviors of Al alloys coated with ENP tested in both air and

3 wt% NaCl. Under the as-plated condition, the coating was approximately composed of 18 wt% P and was 38–40 μm thick. The coated substrate showed an improvement in fatigue properties [82].

5.7 Wettability

The non-wetting surfaces, hydrophobic surfaces, lead to formation of an efficient corrosion protection coating, since they retard the penetration of the corrosive ions to the coated surface. For ENP nanocomposite coatings, the addition of ionic or non-ionic surfactants in an electroless bath enhances the wettability of a coated surface [83]. Using sodium lauryl sulfate (SLS) as a wetting agent, the dispersion of different nanoparticles (Al_2O_3, SiO_2 and ZnO) in an ENP bath was studied by Dhinakaran et al. [84] in addition to its effects on surface roughness, surface morphologies, microhardness levels, and

Fig. 13 Effects of phosphorus content on the thermal expansion coefficient [61]
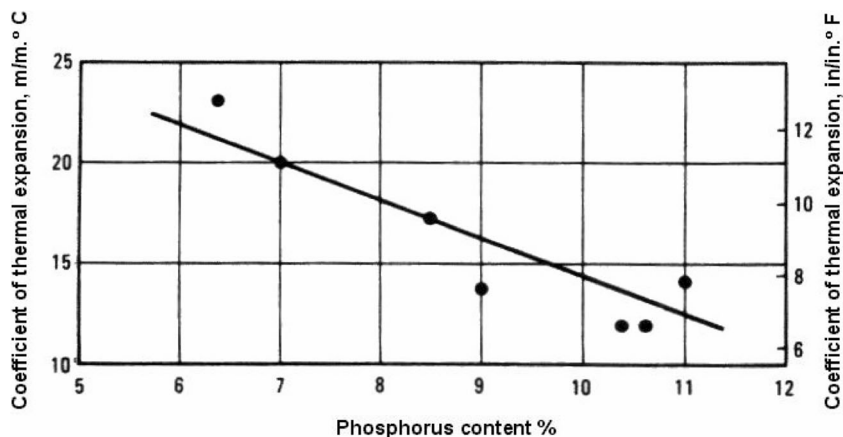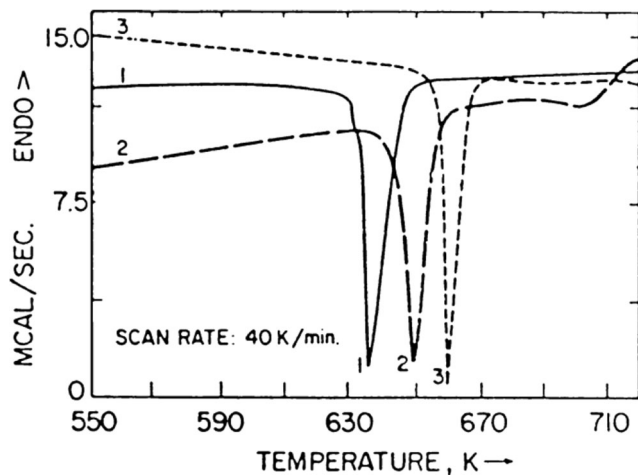
Fig. 14 Differential scanning calorimetry curves of different coatings: 1-Ni-P (11.9 wt% P); 2-Ni-Cu-P (1.7 wt% Cu, 12.2 wt% P); 3-Ni-Sn-P (1.1 wt% Sn, 11 wt% P) [88]

coating to a substrate. To achieve strong adhesion between a coating and substrate, the CTE of the given coating and substrate must be similar. Coating failure mostly occurs as a result of residual thermal stress applied at high working temperatures. ENP coatings are characterized by a variety of thermal expansion coefficients dependent on phosphorus content levels as is shown in Fig. 13 [61]. By controlling phosphorus content levels, residual thermal stress can be reduced. CTE of ENP coatings at 3 wt% phosphorus reaches nearly 22.3 μm/m/°C, whereas they reach 11.1 μm/m/°C at 11 wt% phosphorus [60]. The inclusion of nanoparticles such as Cu and Sn [88] to the ENP matrix-forming nanocomposite increases the crystallization temperature of amorphous Ni–P, in turn improving its thermal stability as is shown in Fig. 14. Enhancing the thermal stability ENP composite coating improves its corrosion resistance.

wear rates. Adding SLS with nanoparticles was found to change the surface morphology of the deposit from unsmooth nodular to smooth, as the surfactant reduced the contact angle and improved the wettability of the Ni-P deposit on the substrate. More investigations of the wettability of ENP and of its composites can be found in [85, 86].

Karthikeyan et al. investigated the effects of heat treatment on the wettability of an ENP coating [87]. Their wettability study showed that as-deposited Ni-P coatings are hydrophobic. Heat treatment at 400 °C changed the hydrophobicity of the ENP coating surface to become hydrophilic as a result of nanocrystalline formation as is shown in Fig. 12.

5.8 Thermal properties

Measurements of the coefficient of thermal expansion (CTE) for any coating are influential, as they affect the adhesion of a

5.9 Wear resistance

Wear involves the gradual deterioration and deformation of contacting surfaces as a result of mechanical action. There are two types of wear: adhesive and abrasive. Adhesive wear occurs when material is lost when hard particles are forced against and move along a solid surface. Abrasive wear occurs between surfaces in frictional contact. As noted above, wear is related to hardness; as hardness is up-surged, wear resistance levels increase. Wear is affected by many factors such as surface hardness; the contact area and its shape; the nature of stress applied; surface morphologies; the type, speed and duration of motion; the temperature; and the form of lubrication. Consequently, as it is difficult to predict and control, wear is a highly complex process. Sahoo studied the optimization of ENP coating process parameters for minimal wear based on an L27 Taguchi orthogonal design with four parameters (bath
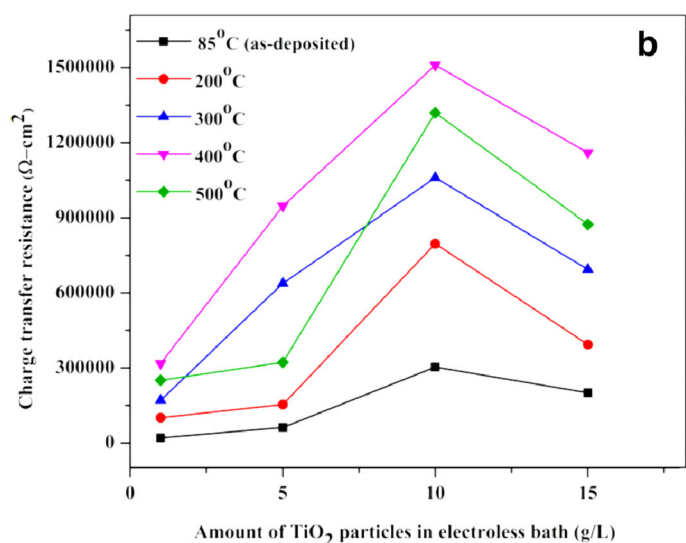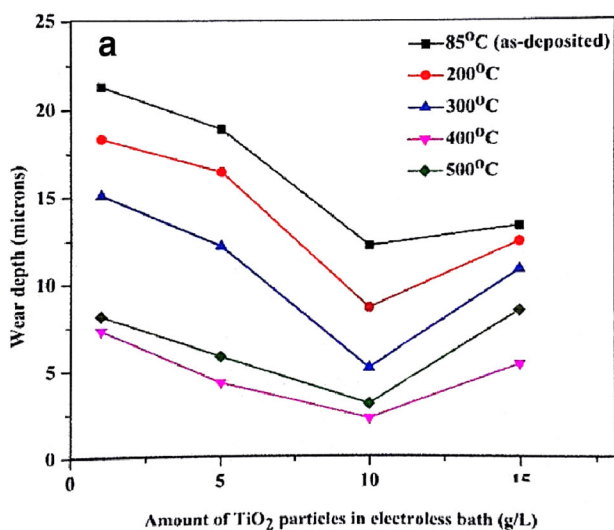

Fig. 15 Effect of annealing temperature and TiO_2 particles on **a** wear depth and **b** corrosion current density [92]
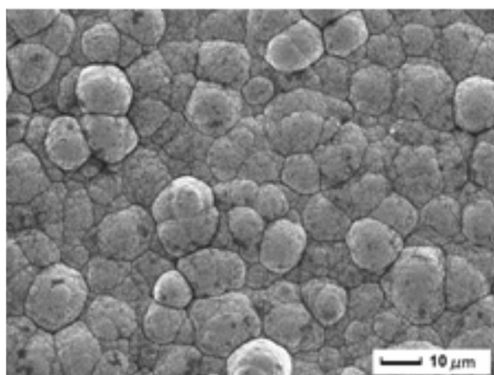
Fig. 16 SEM of the surface morphology of the composite coating [93]
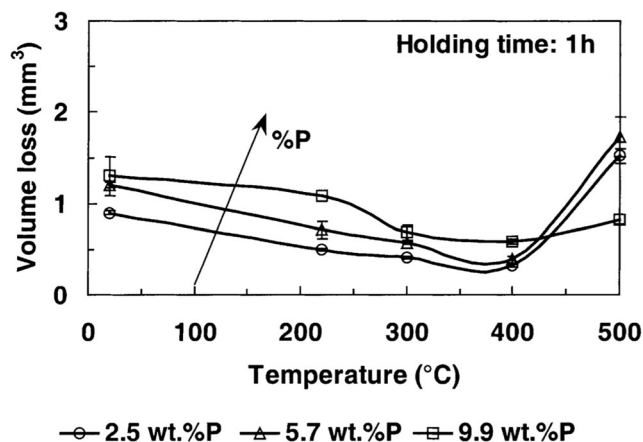

— 2.5 wt.%P — 5.7 wt.%P — 9.9 wt.%P

Fig. 17 Abrasive wear resistance (expressed as volume loss) of Ni-P-SiC coatings as a function of heat treatment temperature and phosphorus content. Applied load, 4.9 N [94]

temperature, nickel concentration, reducing agent concentration, and annealing temperature). It was found that nickel concentrations have a less significant effect in controlling wear properties, whereas the annealing temperature has the most significant effect [89].

Studies have shown that the wear resistance of ENP is enhanced through the addition of different substances to form a composite. ENP-Al_2O_3 nanocomposite was prepared and studied by Li et al. in 2013 [90]. ENP-Al_2O_3 was deposited on carbon steel from a plating bath containing Ni-sulfate, sodium hypophosphite, and Al_2O_3 nanoparticles with different concentrations (0.025, 0.50, 1.00, and 2.00 g L^{-1}). The results showed that the microhardness and wear resistance of the nanocomposite with Al_2O_3 nanoparticles prepared by (i) mechanical milling and (ii) traditional technique (sol gel method) are quite similar. Both properties were enhanced as the Al_2O_3 content was increased, whereas the corrosion resistance in 3.5 wt% NaCl decreased. This is in the contrary to the other study [91], which proved that the presence of 75 g L^{-1} of Al_2O_3 nanoparticles in the coating improved the corrosion resistance of the steel in 3.5 wt% NaCl solution. Therefore, it is assumed that an optimum concentration of Al_2O_3 should be controlled with the nanocomposite in order to have a high corrosion and wear resistance. The presence of TiO_2 in the ENP matrix leads to a significant improvement in the wear resistance, hardness, and corrosion resistance of an ENP deposit [92]. Ni-P-TiO_2 nanocomposite coatings are prepared at different concentrations of TiO_2 particles in the electroless

bath (1, 5, 10, 15 g/L) and annealed at different annealing temperatures (200, 300, 400, and 500 °C). Increasing the titania concentrations and annealing temperatures led to an increase in the wear (decrease in wear depth values) and corrosion (increase in the charge transfer resistance values, R_{ct}) resistances. The minimum wear depth and the highest R_{ct} were obtained after annealing at 400 °C. At a higher annealing temperature (500 °C), the wear depth increased and the R_{ct} decreased compared to these values at 400 °C due to the increase in the grain size of the composite coating and the separation of grains from each other. Figure 15 shows the effect of TiO_2 concentration in the deposition bath on the wear depth and R_{ct} of the ENP-TiO_2 nanocomposite after different annealing temperatures.

The wear resistance of the ENP-SiC nanocomposite coating that deposited on the AZ91D magnesium alloy was enhanced as the concentration of SiC particles in the electroless deposition bath was increased up to a concentration of 4 g L^{-1}. A further increase in the SiC concentration led to a decrease in the microhardness and consequently, the wear resistance of the composite coating [93]. The enhancement of the wear resistance and the microhardness of the composite coating are attributed to the strengthening effect of the SiC and the homogeneous distribution of the SiC particles in the Ni-P matrix, which led to an increase in the compactness of the

Table 3 Coating characteristics

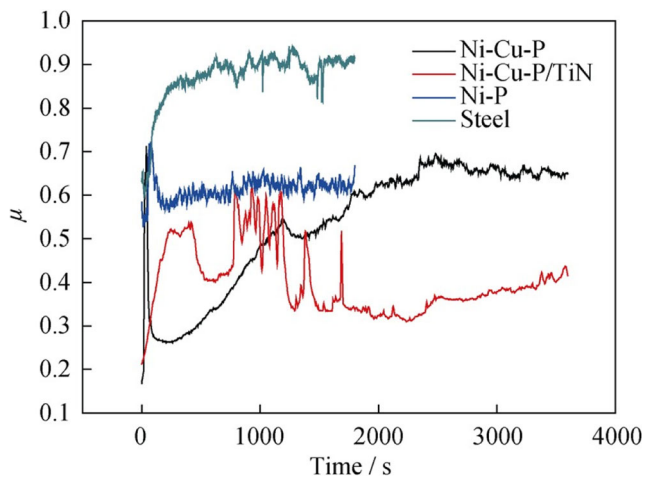| Coating	Phosphorus content (wt%)		SiC concentration in the coated layer (vol%)	Coating thickness (μm)
Ni-P	Low	3.9 ± 0.3		30–60
	Medium	6.0 ± 0.3		
	High	10 ± 0.2		
Ni-P-SiC	Low	2.5 ± 0.8	32 ± 1.0	30–60
	Medium	5.7 ± 0.5	30 ± 2.0	
	High	9.9 ± 1.0	35 ± 1.0	

Fig. 18 Friction coefficients (μ) of steel, Ni–P, Ni–Cu–P, and Ni–Cu–P–TiN [94]

coating, as shown in Fig. 16. Whereas a higher concentration of SiC nanoparticles led to a heterogeneous distribution of the nanoparticles in the coating. In addition, the amount of holes was increased and the integrity of the coatings was reduced which led to a little reduction in the microhardness.

Besides the effect of concentration of the added particle, the heat treatment and the phosphorus content in the composite coating have a significant effect on the wear resistance. A comparative study on the relationships between the structure and abrasive wear resistance of Ni-P-SiC coatings with different phosphorus contents (2.5–10.2 wt.% P) under different heat treatment conditions (300, 400 and 500 °C) was performed [94]. The specifications of the coating are shown in Table 3. The abrasive wear resistance, for low and medium P wt% composite coating, gradually increased up to 400 °C, followed by a severe decrease at 500 °C. The abrasive wear resistance of the coating with high P wt% increased continuously with increasing the annealing temperature up to 300 °C, followed by a relatively stable condition at 400 and 500 °C, as seen in Fig. 17. Increasing the wear resistance of the composite coating is related to the slight grain growth of the Ni-P phase, which has a crystalline structure at low and medium P wt%, approaching a metastable equilibrium at approximately 300 °C and the precipitation of the hard, semi-coherent, Ni_3P phase at approximately 400 °C.
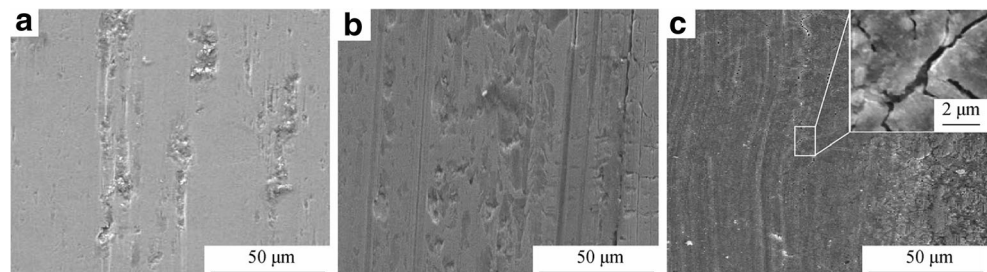
Zhou et al. studied the effects of Cu and TiN in the Ni-Cu-P-TiN ternary nanocomposite on its corrosion and wear resistance [95]. The composite coating is deposited on carbon steel from plating solution containing, in addition to nickel sulfate and sodium hypophosphite, cupric sulfate to increase the corrosion resistance of the composite and TiN particle to enhance the wear resistance. The results showed that the corrosion resistance of the composite coating was doubled relative to that of the ENP coatings, as the incorporation of Cu into the coating enhanced the compact structure by decreasing the number of pores present. In addition, the presence of TiN dramatically increased the wear resistance, as it decreased the friction coefficient of the coating as is shown in Fig. 18. Nevertheless, some cracks formed on the Ni-Cu-P-TiN surface due to stress acting on it and due to internal stress resulting from the incorporation of TiN particles as is shown in Fig. 19c.

There has been a focus on the wear resistance of ENP coatings. This topic is explored at length in [96–100].

5.10 Corrosion resistance

From the above-described properties, ENP coatings exhibit lower levels of porosity and a more uniform thickness and are harder than the equivalent electroplated nickel alloy. These unique properties in addition to their passive nature render ENP deposits superb at resisting corrosion in different environments. Degrees of ENP coating passivity and corrosion resistance are greatly affected by their compositions, i.e., phosphorus content. In neutral and acidic media, the higher (more than 10 wt%) the phosphorus content in coatings, the more resistant coatings will be to corrosion. On the other hand, coatings with less phosphorus content are more resistant to strong alkaline media than coatings with high levels of phosphorus content. Upon being heated to above 220 °C, ENP deposits will form nickel phosphide, which reduces the phosphorus content of the remaining material. Accordingly, the corrosion resistance of coatings is reduced. It has been proven that amorphous alloys are more resistant to corrosion than their crystalline counterparts due to an absence of grain boundaries and due to the formation of glassy films that passivate their surfaces.
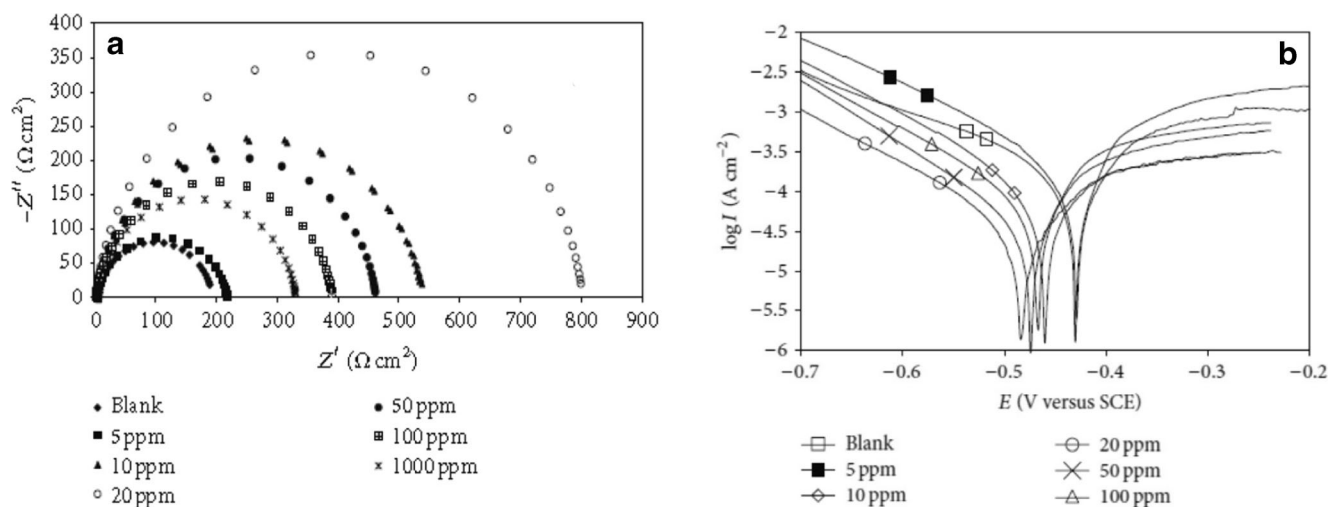
Fig. 19 SEM images of wear-worn surfaces of **a** Ni–P, **b** Ni–Cu–P, and **c** Ni–Cu–P–TiN [95]

Fig. 20 **a** Nyquist and **b** Tafel plots for composite coatings obtained from a plating bath containing different concentrations of nano-Al_2O_3 particles [101]

As noted above, the incorporation of nanoparticles into an ENP coating matrix enhances their properties. Consequently, the corrosion resistance of ENP composite coatings in different environments constitutes their broadest application. Ashassi-Sorkhabi et al. described corrosion resistance of electroless Ni-Cu-P containing nano-Al_2O_3 particles in 0.5 M H_2SO_4 solutions [101]. Ni-Cu-P/Al_2O_3 composite coatings are prepared on mild steel from an alkaline electroless plating containing 1 g L^{-1} $CuSO_4$ and different concentrations of Al_2O_3 nanoparticles (5, 10, 20, 50, 100, and 1000 ppm). It was found that the inclusion of Al_2O_3 nanoparticles improved the corrosion resistance of the examined coating with a maximum achieved at 20 ppm nanoparticle concentration as is shown in Fig. 20a, which presents Nyquist plots for the Ni-Cu-P electroless-plated coatings with and without different concentrations of Al_2O_3 nanoparticles. Nyquist plots, Fig. 20a, shows that an increase in the alumina concentration up to 1000 ppm negatively affects the corrosion resistance that has the lowest value of the charge transfer resistance (R_{ct}). Figure 20b represented Tafel plots of the composite coatings with different concentrations of alumina. The polarization measurements (Tafel plots) are in good agreement with EIS results.

Effects of different concentrations (0.05, 0.10, 0.15, and 0.20 g L^{-1}) of Yb^{3+} on the corrosion resistance and deposition rate of ENP deposits were studied by Yan [102]. The presence of Yb^{3+} resulted in a significant improvement in the corrosion resistance of the coating and accelerated its deposition rate. Increasing Yb^{3+} up to 0.20 g L^{-1}, the corrosion potential, E_{corr}, of the electroless Ni-P coating in 3.5 wt% NaCl solution increased from −0.381 to −0.08 V, and the corrosion current density i_{corr} decreased from 7.36 to 0.62 mA cm^{-2}, as shown in Fig. 21. Enhancing the corrosion resistance of the composite coating is achieved since Yb^{3+} accelerates the nucleation rate

of Ni-P alloy, resulting in compact coatings with fine grains and low porosities, as shown in Fig. 22.

ENP ternary coatings exhibit excellent corrosion and functional properties in acidic and alkaline media. Ternary Ni-Zn-P [103] and Ni-Cu-P [104] nanocomposites have been prepared on steel and Mg alloys, respectively. Their effects on the corrosion resistance of the studied ENP coating were tested in 3.5% NaCl solution using potentiodynamic polarization (Tafel plots) and EIS techniques. The inclusion of Cu or Zn enhanced the deposition rate and the degree of corrosion resistance since they have a coating with refined nodules, uniformity, and low porosity, as shown in Fig. 23a, b), and increased deposition rate. In a parallel study, Zhao et al. found that the addition of 6.5 wt% Cu to an electroless Ni–P–PTFE
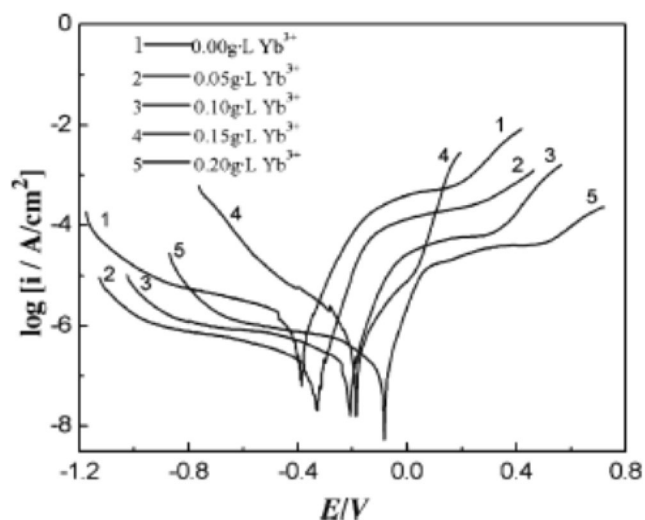

Fig. 21 Polarization curves of electroless Ni–P coatings deposited from the baths with different concentrations of Yb^{3+} in the 3.5 wt% NaCl solution

Fig. 22 Surface morphologies of electroless Ni–P coatings deposited in presence of **a** 0, **b** 0.05, **c** 0.10, **d** 0.15, and **e** 0.20 g L^{-1} Yb^{3+}
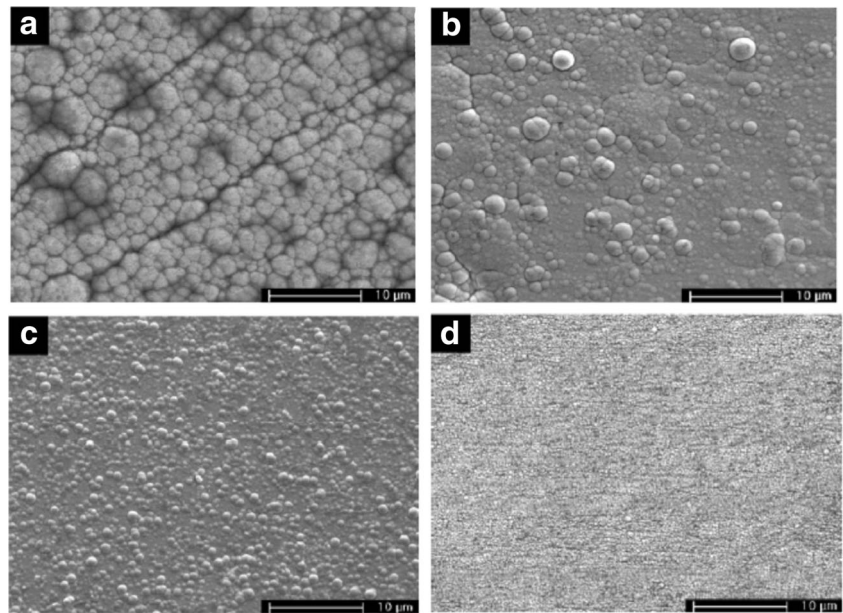

Fig. 23 Surface morphology of **a** Ni-Zn-P [113] and **b** Ni–Cu–P [114] composite coatings
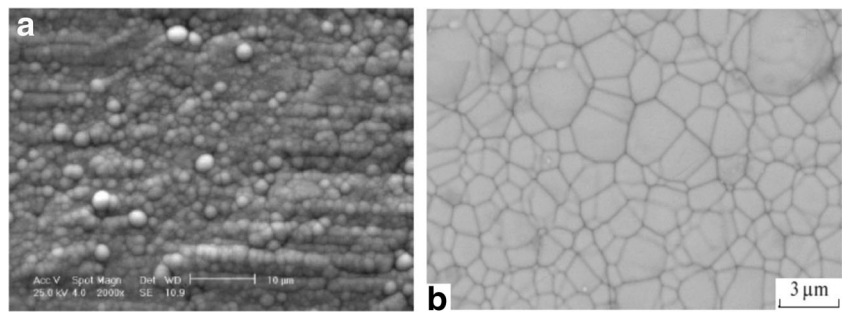
matrix increased the deposition rates and corrosion resistance levels [105].

Unique characteristics of tungsten (e.g., high hardness, tensile strength and melting point values, and a lower linear thermal expansion coefficient) have motivated researchers to develop ternary Ni-W-P alloys as reported in refs. [106–110]. Studies on the corrosion resistance efficiencies of electroless Ni–P–CeO$_2$ and Ni–P–TiO$_2$ composite coatings have been conducted by electrochemical impedance spectroscopy and revealed higher levels of corrosion resistance than those of plain electroless Ni–P deposits [40, 111]. Electroless Ni–P–Fe$_3$O$_4$ composite coatings exhibited higher levels of corrosion resistance than ENP coatings at room temperature in 3.5 wt% NaCl solution [112]. In a recent study, Au coating was deposited on Ni-P coating to improve its efficiency. Furthermore, different organic additives such as polyethylenimine (PEI), hexamethylenetetramine (HET), and benzotriazole (BTA) were added to the deposition bath. The performance of the Au coating was

Fig. 24 Tafel plots of Ni-P with Au deposited from baths with different additives. (a) Ni–P substrate, (b) Ni-P with Au only, (c) with 5 mg L^{-1} HET, (d) 3 mg L^{-1} BTA, and (e) 200 mg L^{-1} PEI

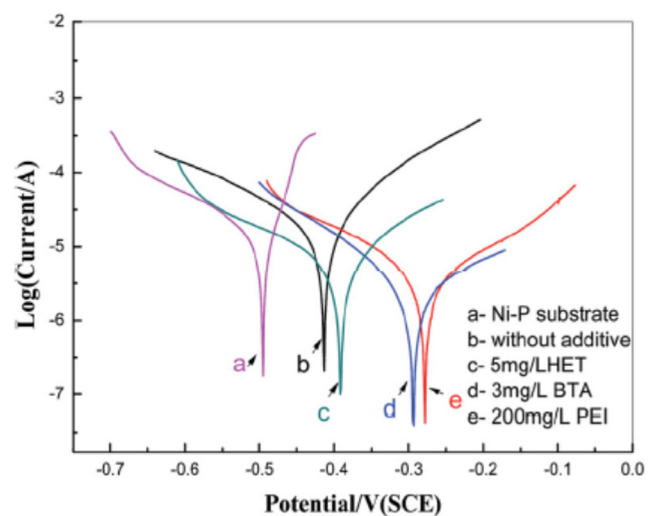**Table 4** Summary of recent advances in the corrosion resistance (CR) studies of the ENP and its nanocomposite coatings including types of substrates used, electroless deposition methods and baths, characterization methods, and major findings

Type of composite	Development methods	ENP bath condition			Characterization techniques	Substrate	Major findings	Ref.
		Temp., $^{\circ}$C	pH	Time (hours)				
Ni-P-SiO$_2$-Al$_2$O$_3$	Addition of SiO$_2$ and Al$_2$O$_3$ nanoparticles of different amounts.	90 ± 1	4.6 ± 0.1	2	SEM, EDX, XRD, EIS, polarization techniques.	6061 Al AZ91HP Mg alloy.	Increasing the number of nanoparticles increases the CR and microhardness of the resulting composite.	[114, 115]
Ni-P-CeO$_2$/RuO$_2$	Reinforcement ENP coating with mixed oxide of CeO$_2$/RuO$_2$.	85 ± 2	4.5	2	SEM, EDX, XRD, AFM, OCP, polarization techniques.	Mild steel.	CeO$_2$/RuO$_2$ were widely distributed across the ENP coating and increased the CR.	[116]
Ni-Co-P	Codeposition with Al$_2$O$_3$, SiN and SiC.	90 ± 5	8	1	SEM, EDX, XRD, PP, EIS, Profilometry.	Al ASC-M20 alloy.	Maximum CR was achieved with an Al$_2$O$_3$ codeposited coating, and the highest degrees of microhardness and wear resistance were achieved when using a SiC codeposited coating.	[117]
Ni-Sn-P	Addition of SnCl$_4$ to an electroless bath.	85~93	4.5~5.5	3	SEM, XRD, PP, EIS.	(CF) steel.	Formation of a homogeneous amorphous alloy layer on CF steel that improves the CR value.	[118]
Ni-P-SiO$_2$	Addition of different amounts of nano-SiO$_2$ (5 to 15 g.L^{-1}).	90 ± 1	4.5 ± 0.1	1.5	FESEM, EDX, PP, EIS.	Al 7075-T6 alloy.	With 12.5 g.L^{-1} SiO$_2$, the coating hardness was enhanced from 453 to 980 VH but the CR value diminished following heat treatment.	[119]
Ni-P-W	Addition of sodium tungstate, tungsten powder, and Ni-P-coated tungsten powder to an ENP bath.	85 ± 2	4.5	2	XRD, SEM, EDS, OCP, EIS.	Mild steel.	The protective barrier created by Ni-P-coated tungsten powder incorporated into ENP coating was found to be the strongest.	[120]
Ni-Cu-P-TiN	Addition of TiN particles to form Ni-Cu-P-TiN composite.	75–80	4.8–5.1	1	PP, SEM, EDX, XRD, Pin-on-disk.	C-steel.	The CR of Ni-Cu-P-TiN was doubled relative to that of ENP.	[95]
Ni-Y-P	Addition of different amounts of Y^{3+} (2–8 mmol/L).	85 ± 2	5 ± 0.1	1	SEM, EDX, PP.	Sintered Nd–Fe–B magnets.	The best CR was obtained at 6 mmol L^{-1} of Y^{3+}.	[121]
Ni-P-SiO$_2$	Formation of a pre-layer of Ni-P followed by the addition of SiO$_2$ nanoparticles.	90	–	1.5–2	FE-SEM, EDS, AFM, EIS.	Cu.	The magnitude of CR was increased and the surface roughness and porosity of the coating were reduced with SiO$_2$ nanoparticle incorporation.	[122]
Ni-P-TiO$_2$	Addition of different amounts of TiO$_2$ nanoparticles.	85	4.5	1	SEM, EDX, XRD, PP, EIS	Low C-steel.	Ni-P-nano-TiO$_2$ coating exhibited superior CR over Ni-P coating.	[123]
Ni-P/Ni-B-B$_4$C	Deposition of duplex composite coatings containing B$_4$C.	80	4.6	–	SEM, EDX, XRD, PP, EIS.	CK45 steel.	The layers are highly compatible. Microhardness levels and the CR of Ni-B-B$_4$C were higher than those of ENP coatings.	[124]
Ni-P-SiC	Incorporation of SiC nanoparticles.	88 ± 2	4.7	2	SEM, EDX, PP, EIS, Pin-on-disk, Vickers tester.	Al 6061 alloy.	SiC nanoparticles enhanced the CR and tribological properties of AA in 3.5 wt% NaCl.	[125]
Ni-P-Cg-TiO$_2$	Codeposition of graphite particles with the Ni-P-TiO$_2$.	80	5	1	SEM, XRD, PP, DSC.	Galvanized C-steel.	The CR value was decreased with the addition of graphite particles (Cg) to the composite Ni-P-TiO$_2$.	[126]
Ni-P/Ni-P-ZrO$_2$	Formation of a double layer of Ni-P with the upper layer including ZrO$_2$.	Outer layer: Temp 80, pH 6–6.4, time 1.5 Inner layer:			SEM, XRD, PP, Salt Spray Test.	Mg AZ31 alloy.	Double-layered Ni-P/Ni-P-XZrO$_2$ coatings	[127]

Table 4 (continued)

Type of composite	Development methods	ENP bath condition			Characterization techniques	Substrate	Major findings	Ref.
		Temp., °C	pH	Time (hours)				
		Temp 80, pH 4.5–5, time 2					can resist salt spray tests for more than 480 h.	
Ni-P/Ni-B-BN	Insertion of BN nanoparticles into the duplex electroless composite coating.	85	4.6	2	SEM, EDX, PP, EIS, XRD, Pin-on-disk test, Vickers tester.	CK45 steel.	The presence of both a Ni-P pre-layer and BN nanoparticles improved the CR of the two-layered composite coating (Ni-P/Ni-B-BN).	[128]
Ni-P-Zn	Enhancing the electroless Ni-P via Zn.	85	10.5	1	SEM, PP, EIS, Salt Spray Test.		CR levels were increased through the optimization of P and Zn content levels.	[129]
Ni-P-Nylon 66	Incorporation of nylon 66 into an ENP.	90 ± 1	4.5 ± 0.02	2	SEM, EDX, FTIR, PP, EIS.	C-steel.	The presence of nylon increased the thickness and corrosive strength of the composite coatings.	[130]
Ni-P-CNT	Uniform distribution of CNT across ENP coatings.	88 ± 2	5.2	0.5	SEM, TEM, AFM, Shear tests.	Cu.	The presence of CNT provided Ni-P-CNT composites with high levels of mechanical strength, CR, and stability.	[131]
Ni-P-WS$_2$	Multilayers of Ni-P and Ni-P-WS$_2$ are constructed and investigated.	87	5.8	5	SEM, XRD, AFM, EIS, Pin- on-disk test, Vickers test.	Al.	The incorporation of WS$_2$ and the existence of Ni$_3$P led to an increase in the CR of the Ni-P-WS$_2$ composite relative to that of the ENP coatings.	[132]
Ni-Co-P	Insertion of SiC particles of different sizes into the composite to form Ni-Co-P-SiC.	90 ± 5	8	1	SEM, EDX, EIS XRD, Vickers hardometer, PP.	Al alloy.	Higher levels of microhardness and corrosion resistance were observed following the addition of less SiC to the Ni-Co-P-SiC.	[133]
Ni-P/Ni-P-PTFE	Ni-P-PTFE coating is supported by a pre-layer of Ni-P coatings.	85 ± 1	4.6~4.8	2	SEM, XRD, Hardness test, Porosity test, Friction coefficient.	Galvanized iron.	Ni-P/Ni-P-PTFE composite coatings exhibit strong substrate bonding, high levels of hardness, low friction coefficients, and high CR values.	[134]
Ni-P-DNP	Incorporation of different quantities of diamond nanoparticles (DNP).	90 ± 5	8	1	SEM, EDX, XRD, PP, EIS.	Mild steel.	DNP significantly improved the CR of the ENP coatings.	[135]
Ni-P-ZnO	Incorporation of ZnO nanoparticles.	88–93	4.5–4.7	3	SEM, EDX, XRD, PP, EIS.	St37 steel.	Adding ZnO nanoparticles shrank the electrochemically active area of the coating, thus increasing the CR.	[136]
Duplex Ni-P Duplex Ni-P-TiO$_2$ Duplex Ni-P-ZrO$_2$	Formation of duplex Ni-P with low levels of P-content in the first layer and with high levels of P content in the second layer followed by the incorporation of ceramic TiO$_2$ and ZrO$_2$ microparticles.	90	6.2	2	SEM, EDX, XRD, PP, EIS.	Mg AZ31 alloy.	All of the coatings generated excellent CR values. The best CR was achieved when using ceramic composite coatings. Advantages of the use of ceramic TiO$_2$ and ZrO$_2$ microparticles can be observed after heat treatment.	[137]
Ni-P-CNT	Inclusion of CNT to form Ni-P-CNT composite and examination of CR in acidic and neutral media.	88 ± 2	4.7	3	SEM, PP, EIS.	Cu.	The incorporation of CNTs into the composite coating significantly increased the CR of electroless Ni–P in both acidic and neutral media.	[138]
Ni-P-Al$_2$O$_3$	Incorporation of different amounts (5–20 g/L) of Al$_2$O$_3$ nanoparticles.	88–90	5.5–8	2	SEM, EDX, PP, XRD, pin-on-disk test.	Mild steel.	The Ni-P- Al$_2$O$_3$ composite coatings acquired higher values of microhardness and CR than those of the ENP coatings. CR values increased as alumina content levels increased.	[139]

Table 4 (continued)

Type of composite	Development methods	ENP bath condition			Characterization techniques	Substrate	Major findings	Ref.
		Temp., °C	pH	Time (hours)				
Ni-P-SiC and Ni-P-CNT	Enforcing a Ni-P coating with either SiC or CNT.	88–93	4.5–4.7	2	SEM, EDX, PP, EIS.	API-5 L X65 steel.	The Ni-P-CNT coating showed the lowest levels of porosity and the highest CR values relative to those of Ni-P-SiC composite coatings.	[140]
Ni-P-kaolin	Codeposition of kaolin nanoparticles with Ni-P coatings.	Different temperatures (40, 50, 60, 70, 80, and 90) at pH 6 for 30 min, different pH values (4, 4.5, 5, 6, 7, 8) at 90 °C for 30 min and different periods (10 to 90 min) at 90 °C and pH 6.			SEM, EDX, XRD, PP, EIS.	Cu, mild steel and stainless steel.	A new bath formulation was developed for producing Ni–P–kaolin. The CR is enhanced through the incorporation of kaolin into the Ni-P matrix.	[141]
Ni-PCTFE-P	Incorporation of polychlorotrifluoro-ethylene nanoparticles into an ENP bath.	90 ± 0.1	4.5	0.5	SEM, EDX, XRD, E_{OCP}, EIS, PP.	Cu.	We observed a significant shift in corrosion potential in the noble direction, a decrease in the corrosion rate, an increase in charge transfer resistance, and a decrease in double-layer capacitance values with the incorporation of PCTFE particles into the Ni-P matrix.	[142]

tested using Tafel polarization in a 3.5% NaCl solution [113]. The results showed that the presence of additives allowed the gold film to increase its corrosion resistance and BTA is more resistant to corrosion than the other inhibitors examined, as shown in Fig. 24. In addition, according to the SEM results, the morphology of immersion gold surface shows a honeycomb structure and the size of Au particles gets smaller, as shown in Fig. 25 [113].

Fig. 25 SEM images of Ni-P with Au with different additives in the bath. **a** Without additive, **b** 200 mg L^{-1} PEI, **c** 3 mg L^{-1} BTA, and **d** 5 mg L^{-1} HET
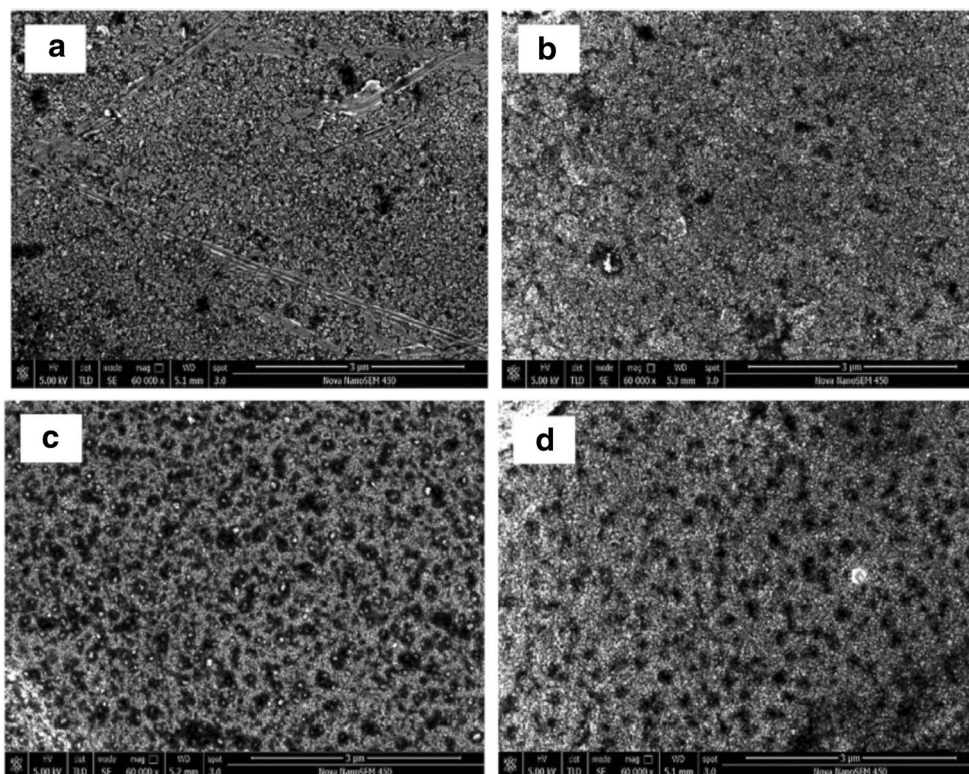
Table 4 summarizes recent preparation of different ENPs and nanocomposite coatings on different substrates and our characterization techniques and applications.

6 Future work on ENP and on its composite coatings

This review article sheds the light on the overall aspects of the electroless nickel-phosphorus (ENP) coatings. It clarifies the mechanisms, electroless bath ingredients, the main requirements of the electroless deposition, and the effect of heat treatment. In addition are the different types of the Ni-P composite coatings and their impact on the properties and characteristics. As a result, ENP coatings and their composite are vital for controlling and mitigating corrosion. Therefore, further electroless research shall be conducted to develop these composite coatings.

In future, complex composite materials such as Ni-P/PTEF/TiO$_2$/ZrO$_2$ or other composite particles such as SiC, CeO$_2$, TiO$_2$, Al$_2$O$_3$, or CNTs can be used to address future needs and to generate composite coatings that protect against corrosion. New methods in terms of corrosion and wear protection can be developed to facilitate the ENP coating of complex substrates such as aluminum and magnesium, which require the use of thick and pore-free coatings.

Furthermore, the use of new nanoparticles such as TiNi or CN in the electroless coating matrix to enhance its strength, hardness, and corrosion, as well as wear resistance, is critical.

Given calls for greener plating technologies, achieving maximum levels of protection and high levels of durability at low prices, will lead to a greater need to apply effective green polymers as second or third phases of ENP coating to ensure a new generation of ENP nanocomposite coatings.

Moreover, increasing the equipment productivity, achieving a maximum efficiency from the bath, developing new plating technologies, using composite materials, and reducing the chemical usage are still in need for research to create new opportunities essential for the future of the ENP coating implementation in corrosion prevention.

Compliance with ethical standards

References

1. A. Wurtz, C. R. Acad. Sci. **18**, 702 (1844)
2. A. Wurtz, C. R. Acad. Sci. **21**, 149 (1845)
3. A. Brenner, G.E. Riddel, Nickel plating on steel by chemical reduction. J. Res. Natl. Bur. Stand. **37**, 31 (1946)
4. V. Mandich, A. Krulik, Met. Finish. **91**, 33 (1993)
5. V.T. Talinn, Finishing. **12**, 26 (1988)
6. R. Weil, J.H. Lee, K. Parker, Plat. Surf. Finish. **76**, 62 (1989)
7. F.B. Mainier, M.M. Araujo, On the effect of the electroless nickel-phosphorus coating defects on the performance of this type of coating in oilfield environments. SPE Adv. Technol. Ser. **2**, 63–67 (1994)
8. F. Delaunois, J.P. Petitjean, P. Lienard, M. Jacob-Duliere, Surf. Coat. Technol. **124**, 201 (2000)
9. X. Liu, J.-Q. Gao, W.B. Hu, Plating & Finishing. **28**, 30 (2006)
10. D. Baudrand, Finishing. **63**, 80 (2009)
11. A. Gould, P.J. Boden, S.J. Harris, Phosphorus distribution in electroless nickel deposits. Surf. Technol. **12**, 93–102 (1981)
12. J. Bielinski, Oberflache Surface. **5**, 423 (1984)
13. W. Riedel, *Electroless Nickel Plating* (Redwood Press Limited, Liverpool, 1991)
14. F.B. Mainier, M.P. Cindra Fonseca, S.S.M. Tavares, J.M. Pardal, J. Mater. Sci. Chem. Eng. **1**, 1 (2013)
15. D. Barker, Electroless deposition of metals. Trans. Inst. Metal Finish. **71**, 121–124 (1993)
16. D.T. Gawne, U. Ma, Structure and wear of electroless nickel coatings. Mater. Sci. Tech. **3**, 228–238 (1987)
17. S. Mordechay, P. Milan, *Modern Electroplating*, fifth edn. (John Wiley & Sons, Inc, 2010)
18. S. Jothi, J. Lian, S. Wei, J. Alloys Compd. **571**, 183 (2013)
19. R.H. Guo, S.X. Jiang, C.W.M. Yuen, M.C.F. Ng, J.W. Lan, G.H. Zheng, Influence of deposition parameters and kinetics of electroless Ni-P plating on polyester fiber. Fibers and Polymers. **13**(8), 1037–1043 (2012)
20. Z. Chen, X. Xiaoda, C.W. Chee, M. Subodh, Effect of plating parameters on the intrinsic stress in electroless nickel plating. Surf. Coat. Technol. **167**, 170–176 (2003)
21. K.H. Krishnan, S. John, K.N. Srinivasan, J. Praveen, M. Ganesan, P.M. Kavimani, Metal. Mater. Trans. **A37**, 1917 (2006)
22. H. Ashassi-Sorkhabi, S.H. Rafizadeh, Surf. Coat. Technol. **176**(3), 318 (2003)
23. M. Yan, H.G. Ying, T.Y. Ma, Surf. Coat. Technol. **202**(24), 5909 (2008)
24. G.O. Mallory, J.B. Hadju, *Electroless Plating: Fundamentals & Applications* (AESF, Orlando, 1991)
25. K.G. Keong, W. Sha, Crystallisation and phase transformation behaviour of electroless nickel-phosphorus deposits and their engineering properties. Surf. Eng. **18**, 329–343 (2002)
26. G. Zhao, Y. Zou, H. Zhang, Z. Zou, Effect Of low-temperature annealing on the properties of Ni-P amorphous alloys deposited via electroless plating. Arch. Metall. Mater. **60**, 865–869 (2015)
27. E. Broszeit, Mechanical, thermal and tribological properties of electro- and chemodeposited composite coatings. Thin Solid Films **95**, 133–142 (1982)
28. K.G. Keong, W. Sha, S. Malinov, Hardness evolution of electroless nickel–phosphorus deposits with thermal processing. Surf. Coat. Technol. **168**, 263–274 (2003)
29. D.T. Gawne, U. Ma, Friction and wear of chromium and nickel coatings. Wear **129**, 123–142 (1989)
30. D. Nava, C.E. Dávalos, A. Martínez-Hernández, F. Manríquez, Y. Meas, R. Ortega-Borges, J. Pérez-Bueno, G. Trejo, Int. J. Electrochem. Sci. **8**, 2670 (2013)
31. I. Apachitei, J. Duszczyk, L. Katgerman, P.J.B. Overkamp, Electroless Ni–P composite coatings: the effect of heat treatment

on the microhardness of substrate and coating. Scr. Mater. **38**, 1347–1353 (1998)

32. A. Grosjean, M. Rezrazi, J. Takadoum, P. Bercot, Hardness, friction and wear characteristics of nickel-SiC electroless composite deposits. Surf. Coat. Technol. **137**, 92–96 (2001)

33. Y.Z. Zhang, Y.Y. Wu, K.N. Sun, M. Yao, J. Mater. Sci. Lett. **17**, 119 (1998)

34. Y.W. Xiang, J.Y. Zhang, C.H. Jin, Plat. Surf. Finish. **88**(2), 64 (2001)

35. J.N. Balaraju, S.K. Seshadri, Preparation and characterization of electroless Ni-P and Ni-P-Si3N4 composite coatings. Trans. Inst. Met. Finish. **77**, 84–86 (1999)

36. Z. Abdel Hamid, M.T. Abou Elkhair, Development of electroless nickel–phosphorous composite deposits for wear resistance of 6061 aluminum alloy. Mater. Lett. **57**, 720–726 (2002)

37. S.M. Moonir-Vaghefi, A. Saatchi, J. Hejazi, Deposition and properties of electroless nickel-phosphorus-molybdenum disulfide composites. Met. Finish. **95**(11), 46–52 (1997)

38. M.D. Ger, B.J. Hwang, Effect of surfactants on codeposition of PTFE particles with electroless Ni-P coating. Mater. Chem. Phys. **76**, 38–45 (2002)

39. I.R. Mafi, C. Dehghanian, Comparison of the coating properties and corrosion rates in electroless Ni–P/PTFE composites prepared by different types of surfactants. Appl. Surf. Sci. **257**, 8653–8658 (2011)

40. G. Jiaqiang, L. Lei, W. Yating, S. Bin, H. Wenbin, Electroless Ni–P–SiC composite coatings with superfine particles. Surf. Coat. Technol. **200**, 5836–5842 (2006)

41. J.N. Balaraju, T.S.N. Sankara Narayanan, S.K. Seshadri, Evaluation of the corrosion resistance of electroless Ni-P and Ni-P composite coatings by electrochemical impedance spectroscopy. J. Solid State Electrochem. **5**, 334–338 (2001)

42. J. Huiming, G. Haihua, A. Felix, M. Aroyave, Journal of Wuhan University of Technology, Materials Science Edition. **25**(5), 734 (2010)

43. P. Tao, M. Mei-Hua, X. Fei-Bo, X. Xin-Quan, XPS and AES investigation of nanometer composite coatings of Ni P ZnX on steel surface (ZnX = ZnSnO3, Zn3(PO4)2, ZnSiO3). Appl. Surf. Sci. **181**, 191–195 (2001)

44. M. Petrova, Z. Noncheva, E. Dobreva, Electroless deposition of diamond powder dispersed nickel–phosphorus coatings on steel substrate. Trans. Inst. Met. Finish. **89**, 89–94 (2011)

45. H. Kahn, M.A. Huff, A.H. Heuer, The TiNi shape-memory alloy and its applications for MEMS. J. Micromech. Microeng. **8**, 213–221 (1998)

46. S. Miyazaki, A. Ishida, Mater. Sci. Eng. **A273-275**, 106 (1999)

47. Z.G. Wei, R. Sandstorm, S. Miyazaki, J. Mater, Sci. **33**, 3743–3749 (1998)

48. Y.Z. Zhang, M. Yao, Studies of electroless nickel deposits with low phosphorus content. Trans IMF **77**(2), 78–83 (1999)

49. J.N. Balaraju, T.S.N. Sankara Narayanan, S.K. Seshadri, Structure and phase transformation behaviour of electroless Ni–P composite coatings. Mater. Res. Bull. **41**, 847–860 (2006)

50. B. Bozzini, C. Martini, P.L. Cavallotti, E. Lanzoni, Wear **225**, 806 (1999)

51. Y.H. Cheng, Y. Zou, L. Cheng, W. Liu, Effect of the microstructure on the properties of Ni–P deposits on heat transfer surface. Surf. Coat. Technol. **203**, 1559–1564 (2009)

52. H. Yang, Y. Gao, W. Qin, Y. Li, Microstructure and corrosion behavior of electroless Ni–P on sprayed Al–Ce coating of 3003 aluminum alloy. Surf. Coat. Technol. **281**, 176–183 (2015)

53. W.C. Sun, P. Zhang, F. Zhang, W.W. Hou, K. Zhao, Microstructure and corrosion resistance of Ni–P gradient coatings. Trans. Inst. Met. Finish. **93**(4), 180–185 (2015)

54. H. Liu, R.X. Guo, Y. Zong, B.Q. He, Z. Liu, Microstructure and corrosion performance of laser-annealed electroless Ni–W–P coatings. Surf. Coat. Technol. **204**(9–10), 1549–1555 (2010)

55. B.S. Geng, W.Y.H. Wei, L.F. Hou, S. Li, Rare Metal Mat. Eng. **38**, 71 (2009)

56. G.L. Zhao, Y. Zou, Y.L. Hao, Z.D. Zou, Corrosion resistance of electroless Ni-P/Cu/Ni-P multilayer coatings. Arch. Metall. Met. **60**, 1003–1008 (2015)

57. S. Sadreddini, Z. Salehi, H. Rassaie, Characterization of Ni–P–SiO2 nano-composite coating on magnesium. Appl. Surf. Sci. **324**, 393–398 (2015)

58. Z. Liu, W. Gao, Int. J. Mod. Phys. **B20**, 4637 (2006)

59. Y.D. He, H.F. Fu, X.G. Li, W. Gao, Microstructure and properties of mechanical attrition enhanced electroless Ni–P plating on magnesium alloy. Scripta Mater. **58**, 504–507 (2008)

60. R.N. Duncan, Plat. Surf. Finish. **83**, 65 (1996)

61. D.W. Baudrand, Metals Hand Book. Eighth ed. (Ohi, USA, 1978)

62. W. Reidel, Electroless Nickel plating. (ASN International, 1997)

63. A.S. Hamada, P. Sahub, D.A. Porter, Indentation property and corrosion resistance of electroless nickel–phosphorus coatings deposited on austenitic high-Mn TWIP steel. Appl. Surf. Sci. **356**, 1–8 (2015)

64. N. Balaraju, K.S. Rajam, Int. J. Electrochem. Sci. **2**, 747 (2007)

65. Y.S. Huang, X.T. Zeng, I. Annergren, F.M. Liu, Development of electroless NiP–PTFE–SiC composite coating. Surf. Coat. Technol. **167**, 207–211 (2003)

66. D. Dong, X.H. Chen, W.T. Xiao, G.B. Yang, P.Y. Zhang, Preparation and properties of electroless Ni–P–SiO2 composite coatings. Appl. Surf. Sci. **255**, 7051–7055 (2009)

67. I. Mohammad, A.M. Rizwan, K. Yasir, K. Rawaiz, A.S. Hany, D.A. Mushtaq, O. Olamilekan, D. Burleigh, J. Mater. Eng. Perform. **24**(12), 4835 (2015)

68. W. Chen, W. Gao, Y. He, A novel electroless plating of Ni–P–TiO2 nano-composite coatings. Surf. Coat. Technol. **204**, 2493–2498 (2010)

69. Y. Liuhui, H. Weigang, Z. Xu, J. Alloys Compd. **509**(10), 4154 (2011)

70. L.T. Shi, J. Hu, L. Fang, F. Wu, X.L. Liao, F.M. Meng, in *Mater. Corros.* Effects of cobalt content on mechanical and corrosion properties of electroless Ni-Co-P/TiN nanocomposite coatings (2016). https://doi.org/10.1002/maco.201608844

71. J.N. Balaraju, K.S. Rajam, Electroless ternary Ni–W–P alloys containing micron size Al2O3 particles. Surf. Coat. Technol. **205**, 575–581 (2010)

72. S. Ranganatha, T.V. Venkatesha, K. Vathsala, Development of electroless Ni–Zn–P/nano-TiO2 composite coatings and their properties. Appl. Surf. Sci. **256**, 7377–7383 (2010)

73. J.N. Balaraju, T.S.N. Sankara Narayanan, S.K. Seshadri, J. Appl. Electrochem. **33**, 807–816 (2003)

74. H. Abdel Salam, M.A. Shoeib, H. Hady, Mater. Lett. **80**, 191 (2012)

75. S.R. Allahkaram, T. Rabizadeh, High corrosion resistance of NI-P/nano-SIO2 electroless composite coatings. Int. J. Modern Phys. Conference Series **5**, 810–816 (2012)

76. S.A. Abdel Gawad, A.M. Baraka, M.S. Morsi, M.S.A. Eltoum, Int. J. Electrochem. Sci. **8**(2), 1722 (2013)

77. O.R. Oloyede, Z. Liu, M. Islam, H. Liu, R.X. Guo, Mater. Sci. Eng. Technol. II. **856**, 103 (2014)

78. A. Araghi, M.H. Paydar, Wear and corrosion characteristics of electroless Ni–W–P–B4C and Ni–P–B4C coatings. Surf. Interfaces. **8**(3), 146–153 (2014)

79. A. Pineiro-Jimenez, C. Villalobos-Gutie'rrez, M.H. Staia, E.S. Puchi-Cabrera, Mater. Sci. Technol. **23**, 253 (2007)

80. A. Pertuz, J.A. Chitty, H. Hintermann, E.S. Puchi, Corrosion-fatigue behavior of an annealed AISI 1045 carbon steel coated

with electroless nickel-phosphorus. J. Mater. Eng. Perform. **8**, 424–428 (1999)

81. E.S. Puchi, M.H. Staia, H. Hintermann, A. Pertus, J. Chitty, Thin Solid Film. **290**, 370 (1996)

82. E.S. Puchi-Cabrera, C. Villalobos-Gutierrez, I. Irausquin, J. La Barbera-Sosa, G. Mesmacque, Fatigue behavior of a 7075-T6 aluminum alloy coated with an electroless Ni–P deposit. Int. J. Fatigue **28**(12), 1854–1866 (2006)

83. B.N. Sahoo, B. Kandasubramanian, A. Thomas, J. Polym. **2013**, 2 (2013)

84. R. Dhinakaran, R. Elansezhian, A.A. Lalitha, Effect of nanoadditives with surfactant on the surface characteristics of electroless nickel coating on magnesium-based composites reinforced with MWCNT. Advances in Tribology. **2013**, 1–10 (2013)

85. Y. Wang, X. Shu, S. Wei, C. Liu, W. Gao, R.A. Shakoor, R. Kahraman, Duplex Ni–P–ZrO2/Ni–P electroless coating on stainless steel. J. Alloy Compd. **630**, 189–194 (2015)

86. Y. Nian, S. Chen, M. Youh, C. Chang, Z. Luo, M. Ger, Int. J. Electrochem. Sci. **11**, 9762 (2016)

87. S. Karthikeyan, L. Vijayaraghavan, Transactions of the IMF. 94:5, 265 (2016)

88. J. Georgieva, S. Armyanov, Electroless deposition and some properties of Ni–Cu–P and Ni–Sn–P coatings. J. Solid State Electrochem. **11**, 869–876 (2007)

89. P. Sahoo, Friction performance optimization of electroless Ni–P coatings using the Taguchi method. J. Phys. D Appl. Journal of Phys. **41**, 095305 (2008)

90. C. Li, Y. Wang, Z. Pan, Wear resistance enhancement of electroless nanocomposite coatings via incorporation of alumina nanoparticles prepared by milling. Mater. Design **47**, 443–448 (2013)

91. A.S. Hamdy, M.A. Shoeib, H. Hady, O.F.A. Salam, Corrosion behavior of electroless Ni–P alloy coatings containing tungsten or nano-scattered alumina composite in 3.5% NaCl solution. Surf. Coat. Technol. **202**, 162–171 (2007)

92. P. Gadhari, P. Sahoo, Surf. Rev. Lett. **22**, 1550082 (2015)

93. X.L. Ge, D. Wei, C.J. Wang, Z. Bing, Z.C. Chen, Appl. Mech. Mater. **66**, 1078 (2011)

94. I. Apachitei, F.D. Tichelaar, J. Duszczyk, L. Katgerman, The effect of heat treatment on the structure and abrasive wear resistance of autocatalytic NiP and NiP–SiC coatings. Surf. Coat. Technol. **149**, 263–278 (2002)

95. H.M. Zhou, Y. Jia, J. Li, S.H. Yao, Rare Met. DOI (2016). https://doi.org/10.1007/s12598-015-0663-6

96. W. Rongguang, N. Suketsuku, S. Hiroki, Proceedings of the Pacific Rim International Congress on Advanced Materials and Processing, 8th. Waikoloa, HI, United States. Aug. 4–9, 2013, 1409–1416 (2013)

97. L. Yamin, V. Xing, W. Amin, L. Hongjun, Advanced Materials Research, (Durnten-Zurich, Switzerland). 988, (Material, Mechanical and Manufacturing Engineering II), 117 (2014)

98. G. Zhiming, Z. Song, W. Ying, W. Xin, W. Lijuan, Int. J. Electrochem. Sci. **10**, 637 (2015)

99. L. Naiming, Z. Peng, Z. Jiaojuan, X. Faqin, T. Bin, J. Wuhan Univ. Technol. Mat. Sci. Edit. **30**, 622 (2015)

100. L. Junming, W. Dandan, C. Hui, W. Aijuan, Z. Jumei, Surf. Coat. Technol. **279**, 9 (2015)

101. H. Ashassi-Sorkhabi, H. Aminikia, R. Bagheri, Int. J. Corros. **2014**, 1 (2015)

102. M. Yan, H.G. Ying, T.Y. Ma, W. Luo, Effects of Yb3+ on the corrosion resistance and deposition rate of electroless Ni–P deposits. Appl. Surf. Sci. **255**, 2176–2179 (2008)

103. I. Constantin, Microstructural characterization and corrosion behavior of electroless Ni-Zn-P thin films. J. Metall. **2014**, 1–6 (2014)

104. Z. Rajabalizadeh, D. Seifzadeh, The effect of copper ion on microstructure, plating rate and anticorrosive performance of electroless Ni-P coating on AZ61 magnesium alloy. Prot. Met. Phys. Chem. Surf. **50**(4), 516–523 (2014)

105. Q. Zhao, Y. Liu, E.W. Abel, Effect of Cu content in electroless Ni–Cu–P–PTFE composite coatings on their anti-corrosion properties. Mater. Chem. Phys. **87**, 332–335 (2004)

106. A. Nikitasari, E. Mabruri, (2015) The 3rd International Conference on Advanced Materials Science and Technology (ICAMST 2015). AIP Conf. Proc. 1725, 020053-1-020053-11. doi: https://doi.org/10.1063/1.4945507

107. L. Hong, L. Michael, B. Yashar, M. Yongsheng, Z. Hongbo, L. Jing-Li, Surf. Coat. Technol. **277**, 99 (2015)

108. Z. Chunmei, Y. Yingwu, Anti-Corros. Methods Mater. **61**(5), 314 (2014)

109. S.V. Ezhil, C. Purba, S. Subramanian, J.N. Balaraju, Surf. Coat. Technol. **240**, 103 (2014)

110. R. Supriyo, S. Prasanta, Portug. Electrochim. Acta. **30**(3), 203 (2012)

111. H.M. Jin, S.H. Jiang, L.N. Zhang, Microstructure and corrosion behavior of electroless deposited Ni–P/CeO2 coating. Chin. Chem. Lett. **19**, 1367–1370 (2008)

112. A.A. Zuleta, O.A. Galvis, J.G. Castano, F. Echeverria, F.J. Bolivar, M.P. Hierro, F.J. Perez-Trujillo, Preparation and characterization of electroless Ni–P–Fe3O4 composite coatings and evaluation of its high temperature oxidation behaviour. Surf. Coat. Technol. **203**, 3569–3578 (2009)

113. Y. Wang, H. Liu, S. Bi, M. He, C. Wang, L. Cao, Effects of organic additives on the immersion gold depositing from a sulfite–thiosulfate solution in an electroless nickel immersion gold process. RSC Adv. **6**, 9656–9662 (2016)

114. S. Rahemi Ardakani, A. Afshar, S. Sadreddini, A.A. Ghanbari, Characterization of Ni-P-SiO 2 -Al 2 O 3 nano-composite coatings on aluminum substrate. Mater. Chem. Phys. **189**, 207–214 (2017)

115. S. Sadreddini, S. Rahemi Ardakani, H. Rassaee, Corrosion behavior and microhardness of Ni-P-SiO2-Al2O3 nano-composite coatings on magnesium alloy. J. Mater. Eng. Perform. **26**(5), 2032–2039 (2017)

116. S.M.A. Shibli, A.H. Riyas, M. Ameen Sha, R. Mole, Tuning of phosphorus content and electrocatalytic character of CeO 2 -RuO 2 composite incorporated Ni-P coating for hydrogen evolution reaction. J. Alloys Compd. **696**, 595–603 (2017)

117. J. Hu, L. Fang, X.-L. Liao, L.-T. Shi, Surface Engineering. (2016). https://doi.org/10.1080/02670844.2016.1230975

118. L. Junyan, Y. Jie, F. Weijie, L. Qingchao, Z. Qian, Z. Xiaodong, Int. J. Electrochem. Sci. **11**(2), 899 (2016)

119. S. Sadreddini, A. Afshar, The effect of heat treatment on properties of Ni–P–SiO2 nano-composite coating. Prot. Met. Phys. Chem. Surf. **52**(3), 492–499 (2016)

120. S.M.A. Shibli, K.S. Chinchu, Development and electrochemical characterization of Ni-P coated tungsten incorporated electroless nickel coatings. Mater. Chem. Phys. **178**, 21–30 (2016)

121. Z.H. Wang, L.L. Zhang, H. Ni, S.J. Wang, Effects of Y3+on properties of electroless NiYP coatings. Surf. Eng. **32**(5), 385–390 (2016)

122. M. Islam, M.R. Azhar, N. Fredj, T.D. Burleigh, O.R. Oloyede, A.A. Almajid, S.I. Shah, Influence of SiO 2 nanoparticles on hardness and corrosion resistance of electroless Ni–P coatings. Surf. Coat. Technol. **261**, 141–148 (2015)

123. M.A. Shoeib, M.M. Kamel, S.M. Rashwan, O.M. Hafez, Corrosion behavior of electroless Ni-P/TiO2nanocomposite coatings. Surf. Interface Anal. **47**(6), 672–680 (2015)

124. M. Rezagholizadeh, M. Ghaderi, A. Heidary, S.M.M. Vaghefi, Electroless Ni-P/Ni-B-B4C duplex composite coatings for improving the corrosion and tribological behavior of Ck45 steel. Prot. Met. Phys. Chem. Surf. **51**(2), 234–239 (2015)

125. R. Soleimani, F. Mahboubi, M. Kazemi, S.Y. Arman, Corrosion and tribological behaviour of electroless Ni–P/nano-SiC composite coating on aluminium 6061. Surf. Eng. **31**(9), 714–721 (2015)

126. S. Liu, X. Bian, J. Liu, C. Yang, X. Zhao, J. Fan, K. Zhang, Y. Bai, H. Xu, Y. Liu, Structure and properties of Ni–P–graphite (Cg)–TiO2composite coating. Surf. Eng. **31**(6), 420–426 (2015)

127. X. Shu, Y. Wang, C. Liu, A. Aljaafari, W. Gao, Double-layered Ni-P/Ni-P-ZrO 2 electroless coatings on AZ31 magnesium alloy with improved corrosion resistance. Surf. Coat. Technol. **261**, 161–166 (2015)

128. A. Baibordi, K. Amini, M.H. Bina, A. Dehghan, Kovove Materialy. **52**(5), 263 (2014)

129. A. Kordijazi, Electrochemical Characteristics of an Optimized Ni-P-Zn Electroless Composite Coating. Adv. Mater. Res. **1043**, 124–128 (2014)

130. M. Jayaraj, A. Siddharthan, Characterization of electroless nickel phosphorus nylon 66 composite coating on low carbon steel. Adv. Mater. Res. **984-985**, 502–507 (2014)

131. S. Xu, X. Hu, Y. Yang, Z. Chen, Y.C. Chan, J. Mater. Sci. Mater. Electron. **25**(6), 2682 (2014)

132. S. Karthikeyan, P.A. Jeeva, N. Arivazhagan, V. Umasankar, K.N. Srinivasan, M. Paramasivam, Wear, hardness and corrosion resistance characteristics of tungsten sulfide incorporated electroless Ni-P coatings. Procedia Engineering **64**, 720–726 (2013)

133. J. Hu, L. Fang, P-W. Zhong, Mater. Manuf. Process. 28(12), 1294 (2013), Effect of reinforcement particle size on fabrication and properties of composite coatings, 1300

134. J.Y. Hou, S.R. Wang, Z.W. Zhou, The effect of Ni-P alloy pre-plating on the performance of Ni-P/Ni-P-PTFE composite coatings. Key Eng. Mater. **561**, 537–541 (2013)

135. H. Ashassi-Sorkhabi, M. Es'haghi, Corrosion resistance enhancement of electroless Ni–P coating by incorporation of ultrasonically dispersed diamond nanoparticles. Corr. Sci. **77**, 185–193 (2013)

136. S.R. Allahkaram, R. Faezi Alivand, M.S. Bakhsh, Iran. J. Mater. Sci. Eng. **10**(1), 10 (2013)

137. E. Georgiza, J. Novakovic, P. Vassiliou, Characterization and corrosion resistance of duplex electroless Ni-P composite coatings on magnesium alloy. Surf. Coat. Technol. **232**, 432–439 (2013)

138. M. Alishahi, S.M. Hosseini, S.M. Monirvaghefi, A. Saatchi, Mater. Corr. **64**(3), 212 (2013)

139. A. Sharma, A.K. Singh, Electroless Ni-P and Ni-P-Al2O3 nano-composite coatings and their corrosion and wear resistance. J. Mater. Eng. Perform. **22**(1), 176–183 (2013)

140. A. Zarebidaki, S-R. Allahkaram, Surf. Eng. 28(6), 400 (2012), Porosity measurement of electroless Ni–P coatings reinforced by CNT or SiC particles, 405

141. K.N. Srinivasan, Pr. Thangavelu, Trans. Inst. Met. Finish. 90(2), 105 (2012)

142. M.G. Hosseini, M. Abdolmaleki, S. Ashrafpoor, R. Najjar, Deposition and corrosion resistance of electroless Ni-PCTFE-P nanocomposite coatings. Surf. Coat. Technol. **206**(22), 4546–4552 (2012)